Comparative Auroral Physics: Earth and Other Planets

Barry Mauk

The Johns Hopkins University Applied Physics Laboratory, Laurel, Maryland, USA

Fran Bagenal

Laboratory for Space and Atmospheric Sciences, University of Colorado, Boulder, Colorado, USA

Here we review selected similarities and differences between the structures and processes associated with the generation of the aurora of strongly magnetized planets within the solar system. Our ultimate objective is to use a comparative approach to determine which aspects of auroral phenomena represent universal features and which aspects are particular to the special conditions that prevail at any one planet. We begin by providing a high-level review of selected fundamental auroral processes operating at Earth as a precursor to discussing selected similar processes and regions at other planets. We then discuss the broad characteristics of the space environments of different planets (Earth, Jupiter, Saturn, Uranus, and Neptune) with an eye toward determining the factors that dictate similarities and differences between the respective auroral systems. With a focus on discrete auroral processes, we finally discuss comparisons between the different systems on the basis of (1) magnetospheric current systems, (2) mechanisms of current closure within the distant regions of the magnetospheres, (3) particle acceleration, (4) ionospheric feedback, and (5) satellite systems.

1. INTRODUCTION

A central question of planetary space science in general and auroral physics in particular is: What aspects are universal and what aspects are specific to the conditions that prevail at any one planet? Universal aspects are those that one might invoke when addressing any distant astrophysical system. In general, the processes generating the most intense aurora represent the most powerful means by which energy and momentum are transported between a planet's space environment, or magnetosphere, and its upper atmosphere and ionosphere. At Jupiter, for example, such processes cause Jupiter's distant space environment to spin up to substantial fractions of the planetary corotational angular rates out to distances as large as 100 Jovian radii, while at the same time causing Jupiter to shed tiny amounts of angular momentum. To the extent that such processes can be invoked over broad parametric states, it is not too great a stretch to conclude that such processes may be involved with the shedding of angular momentum in other distant astrophysical settings, for example, during the periods of planetary formation when magnetic fields still hold sway within the collapsing clouds [e.g., *Mauk et al.*, 2002a].

Findings achieved over the last several decades have revealed that, at least superficially, auroral processes are indeed universal in the sense of being active over a broad spectrum of planetary systems (see Earth, Jupiter, Saturn, and Uranus in Figure 1; see also chapters in this monograph on aurorae on Mars by *Brain and Halekas* [this volume], at Jupiter by *Clarke* [this volume], and at Saturn by *Bunce* [this volume]). Small systems like the Earth that are driven by the solar wind (the wind of ionized gases emanating from the Sun), large

Auroral Phenomenology and Magnetospheric Processes: Earth and Other Planets
Geophysical Monograph Series 197

10.1029/2011GM001192

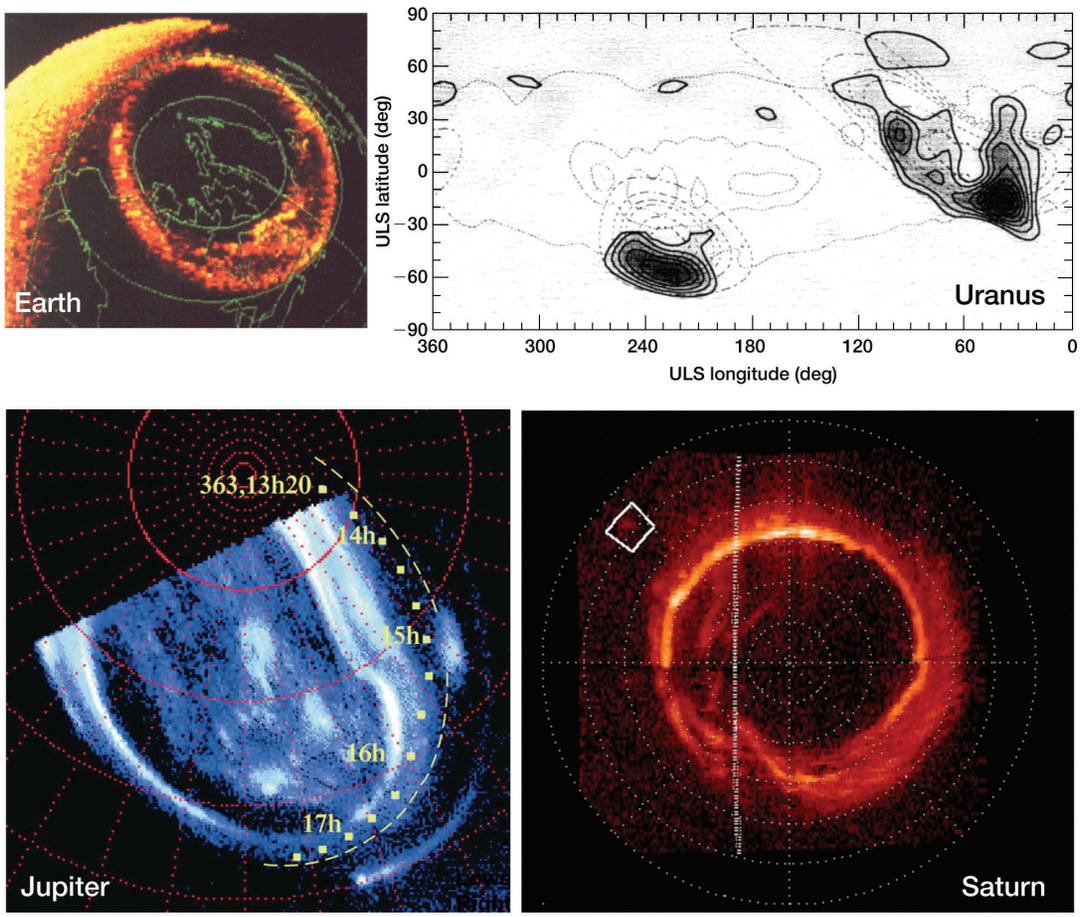

Figure 1. Selected auroral UV images from the Earth (Polar Spacecraft [*Frank and Craven*, 1988], Jupiter (Hubble [from *Mauk et al.*, 2002b] [see *Clarke*, this volume]), Saturn (Cassini Ultraviolet Imaging Spectrograph Subsystem (UVIS) [from *Pryor et al.*, 2011]), and Uranus [*Herbert and Sandel*, 1994; *Herbert*, 2009]). For Jupiter and Saturn, there are planetary latitude lines for both images at 10° latitude intervals. The Uranus image shows a completely different projection and therefore is difficult to compare with the others. However, the symmetry with respect to the magnetic poles can be ascertained by comparisons with the dashed contours, which show the projected positions of the magnetospheric L values, specifically $L = 2$, 3, 4, 5, 10, 20, and 30 R_U. This image comprises a synthesis of Voyager measurements of the UV aurora. Peak emission intensities are less than 500 R.

rotationally driven systems like that of Jupiter, and systems like Saturn with space environments dominated by neutral gas, all have revealed dramatic rings of auroral emissions encircling the magnetic polar axes (Figure 1). While the sizes, power levels, and parametric states of these systems are dramatically different (Table 1) [*Bagenal*, 2009], similarities persist even when the focus is on the details of the planet/space-environment interactions.

In this introduction, we begin by examining some of the fundamental physical processes and regions that have been identified within the Earth's auroral system to set the stage for discussing other planets. The first two sections (sections 1.1 and 1.2) focus on the processes that generate just one type of aurora, discrete aurora, which represents the most intense and structured aurora and which requires active particle acceleration along the magnetic field lines. Discrete aurora is also where the major fraction of our focus is with the comparisons between different planets. Other types of aurora are discussed and placed into context in section 1.3.

Because the sampling of processes acting at other planets is so sparse, we depend substantially on our understanding of the Earth auroral processes to make judgments about what is happening on these other planets. A phenomenon that has received substantial renewed attention over the last decade, and which garnered controversial discussion at the Chapman Conference from which this volume was initiated, is the

Table 1. Selected Parameters Regarding the Planets of the Solar System [*Bagenal*, 2009]

	Earth	Jupiter	Saturn	Uranus	Neptune
Distance from Sun (AU)	1	5.2	9.5	19	30
Radius (km)	6373	71,400	60,268	25,600	24,765
Spin period (sidereal day)	0.997	0.41	0.44	−0.72	0.67
∠(S, N-Ecliptic) (deg)	23.5	3.1	26.7	97.9	29.6
Surface field (nT)	30,600	430,000	21,400	22,800	14,200
Dipole tilt (deg)	9.92	−9.4	~0.0	−59	−47
Magnetopause location (R_p)	8–12	63–92	22–27	18	23–26
Nominal IMF (nT)	8	1	0.6	0.2	0.1
Nominal solar wind density (1 cm^{-3})	7	0.2	0.07	0.02	0.006
Auroral Emission Power (W)	10^{10}	10^{12}	10^{11}	5×10^9	$2–8 \times 10^7$
Open magnetic flux (GWb)	0.5–1	250–720 (model)	15–50		

"Alfvénic aurora." This auroral process is thought to be powered by electromagnetic waves, specifically Alfvén waves that propagate with periods of seconds to tens of seconds within the ionized gases or plasmas that connect the distant magnetosphere to the polar ionosphere (it is understood that even quasi-static auroral structures may be mediated by Alfvén waves with much longer periods). Controversies about this dynamic auroral contribution to the Earth's aurora are similar to discussions that have taken place about the relative roles of turbulence and quasi-static sources of auroral energies at Jupiter, as we shall discuss. Because of that connection, and also because of our perception of gaps in the present literature concerning this topic, we spend some time in section 1.2 discussing the possible relative roles of quasi-static and Alfvén wave sources of auroral power transmission at Earth. In section 2, we make direct comparisons between the auroral processes at Earth and other planets, with a focus on discrete auroral processes.

1.1. Strong Auroral Coupling Processes Revealed at Earth

Figure 2 (after *Lundin et al.* [1998]) provides a traditional view of the generation of discrete auroral discharge phenomena consisting of (1) the generation of electrical currents and voltages within the magnetized plasma that comprise the distant magnetosphere, (2) the diversion of those electrical currents along magnetic field lines toward the polar auroral regions, (3) the generation of impedances and parallel electric fields along the magnetic field lines at low altitudes to midaltitudes as a result of the sparsity of charge carriers in the regions just above the ionosphere, (4) the acceleration of charged particles out of the regions of parallel impedance onto the upper atmosphere and out into the distant magnetosphere, (5) the excitation and ionization of atoms and molecules within the upper atmosphere by the accelerated electrons resulting in strong auroral emissions and enhancements in the electrical conductivity of the ionosphere, (6) the closure of the upgoing and downgoing electric current through the partially conducting ionosphere, and (7) the associated heating through ohmic dissipation of the upper atmosphere and the generation of upper atmospheric winds through the collision of current-carrying ions and neutral atmospheric constituents (see *Mauk et al.* [2002a] for a more detailed discussion of Figure 2).

Multiple processes have been invoked for the generation of the midaltitude impedances and parallel electric fields along magnetic fields [e.g., *Borovsky*, 1993; *Lysak*, 1993] (section 4 of this volume), including stationary electrostatic shock-like structures called double layers, larger-scale electric fields supported by magnetic mirror effects that arise because of the converging magnetic field lines, anomalous

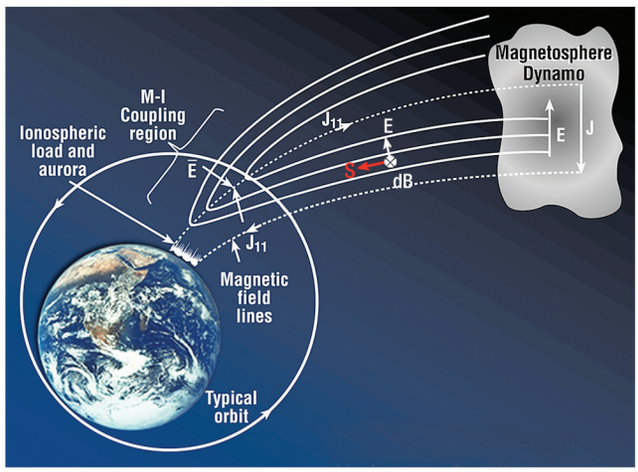

Figure 2. Schematic of the Earth's auroral magnetosphere-ionosphere coupling circuit showing the three key regions and a Freja or FAST spacecraft-like orbit used to sample the midaltitude coupling region. After *Lundin et al.* [1998].

resistivity caused by particle interactions with various wave modes, and parallel electric fields that arise from Alfvén waves propagating at large angles to the magnetic field. Some of these mechanisms are intrinsically time dependent, contrary to the "static" representation given in Figure 2.

1.2. Auroral Energy Flow at Earth

One of the intrinsically time-dependent mechanisms that has received substantial recent attention is the so-called Alfvén wave generator [*Wygant et al.*, 2000; *Keiling et al.*, 2002, 2003; *Watt and Rankin*, this volume]; this process is nicely illustrated in the Figure 1 of *Wygant et al.* [2000]. Reviews on the importance of Alfvén waves generally in auroral and magnetospheric phenomena are provided by *Stasiewicz et al.* [2000] and *Keiling* [2009]. Because the Alfvén wave generator concept has not been reviewed in the context of comparative magnetospheres, and because the argument for supporting the importance of this mechanism is commonly used in the context of planetary magnetospheres, specifically comparing quantitatively the source and dissipation of energy, we spend some time discussing it here.

Alfvénic auroral processes were invoked on the basis of the observation of earthward propagating Alfvén waves at radial distances of 4 to 6 Earth radii (R_E), but at latitudes that map magnetically to the vicinity of the outer boundaries of the population of plasmas that reside within the interior of the antisunward, comet-like magnetic tail of the Earth's magnetosphere, called the plasma sheet. Alfvén wave events are observed with earthward energy fluxes from several to ~100 ergs cm^{-2} s^{-1} when those power density values are mapped (with the funneling amplification associated with the convergence of the magnetic field lines) to auroral altitudes [*Wygant et al.*, 2000; *Keiling et al.*, 2002, 2003]. The energy transport is by means of the Poynting vector, represented in Gaussian units as $\mathbf{S} = (c/4\pi) \cdot \mathbf{dE} \times \mathbf{dB}$, where **dE** and **dB** are the wave fields of the observed parallel-propagating Alfvén waves (note: we will denote the magnitude of the Poynting vector as simply the Poynting flux and will denote the area-integrated energy transport rate as the Poynting fluence). These power density levels, again levels achieved after amplification by the substantial funneling of the magnetic field lines, are compared with the power densities associated with the electron distributions that are observed to generate discrete auroral emissions. *Keiling et al.* [2003] concluded that a substantial fraction (although not all) of the discrete auroral energy dissipations may be powered by these fluctuating Alfvén waves.

A weakness in this conclusion is that this source of energy has not been properly compared with competitive sources of energy, only with the dissipation of energy at the near-Earth "footprints" of the aurora. For a single striking Alfvén wave event, *Wygant et al.* [2002] performed a direct comparison between the Poynting vector magnitudes associated with the static field-aligned electric currents and those values associated with the propagating Alfvén waves, again in the vicinity of the boundary of the plasma sheet populations. These authors showed that the wave-carried Poynting vector magnitude was 1 to 2 orders of magnitude greater than that associated with the more static currents and fields. This comparison has limited value in deciding between the different auroral power sources, however, because the Poynting fluence traditionally thought to be associated with the static-current generation of discrete aurora likely propagates through a different region of space than that associated with the observed Alfvén waves.

Because a proper "apples to apples" comparison between Alfvén wave energy sources and other sources of energy for the discrete aurora has not been presented, it is instructive to examine the flow of energy associated with static currents and fields traditionally thought to be associated with auroral acceleration. Indeed, that energy is also carried by a Poynting flux vector, but a static version (elaborated by *Kelley et al.* [1991]). What is important to recognize is that outside of the regions of power generation and power dissipation, most of the Poynting fluence is not colocated with the field-aligned currents that propagate from the magnetospheric generator to the auroral ionosphere. That Poynting fluence resides between the two current sheets that carry the upward and downward currents. The nonintuitive nature of this finding is discussed, for example, by *Feynman et al.* [1964], who also points out that the Poynting vector representation of energy flow is not unique. However, it is the representation that has been adopted overwhelmingly by the space science community. Within the context of the Poynting vector representation, the validity of where the energy flow takes place can be demonstrated with the simple thought experiment shown in Figure 3a. With this configuration, we generally "bookkeep" the energy dissipation within the resistors (R) as: $P = I \cdot V = V^2/R$, where P is the power dissipation per meter along the x direction (into the page), I is the current per meter in the x direction, R is the electrical resistance per meter along the x-direction, and V is the voltage. But the energy is actually carried by the Poynting fluence that flows between the two plates. One may simply construct the Poynting vector ($c\mathbf{E} \times \mathbf{B}/4\pi$) using the techniques of elementary electricity and magnetism (Gausses law and Ampere's law) to get $\mathbf{E} = -\mathbf{z}V/d$ and $\mathbf{B} = \mathbf{x}(4\pi/c)I$, where (**x**, **y**, **z**) are the unit vectors that form the Cartesian coordinate system. By integrating this Poynting flux across the area between the two plates formed by $A = L \cdot d$, where L is the unit distance of integration along the x direction, one finds that indeed $P = I \cdot V = V^2/R$, just as we found with our bookkeeping formula.

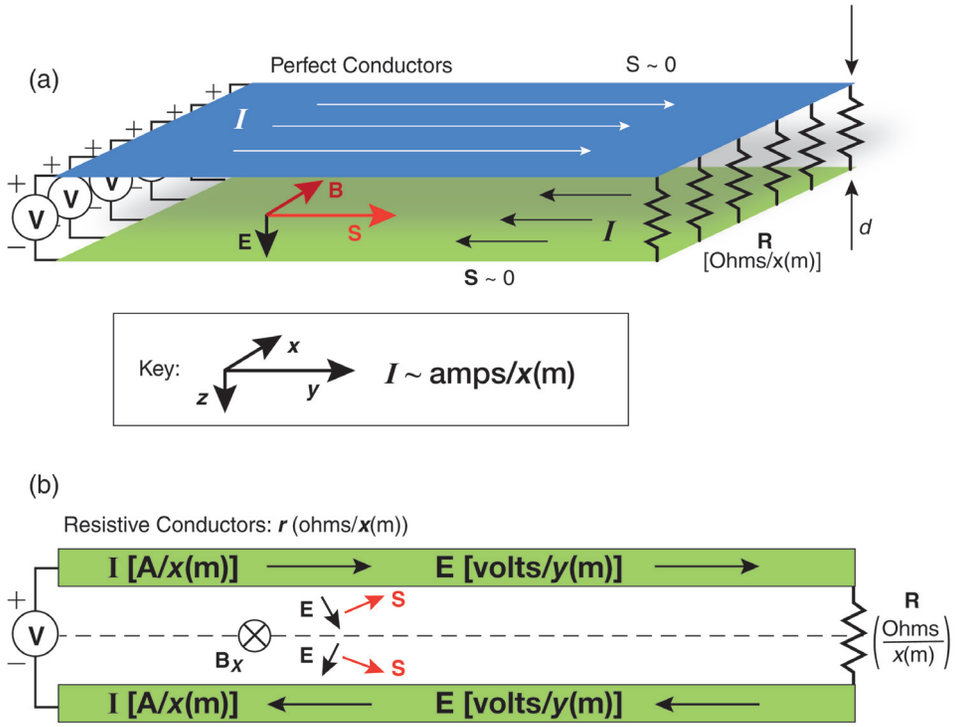

Figure 3. Thought experiments designed to help understand the flow of energy associated with static auroral current systems. See text for details.

The way in which the static current system provides power to the auroral acceleration process is illustrated in Figure 3b, which shows the system examined in Figure 3a, but viewed edge-on. In this case, we also consider current-carrying plates that have some electrical resistance to them. Here one sees that the Poynting flux now no longer flows parallel to the plates but flows across the surface at an angle and into the resistive plates. The plates will heat up in association with the dissipation of electric power, but the flow of energy that provides this heat energy is, within the framework that we have chosen, the Poynting flux that flows through the sides of the plates, not the flow of energy along the current-carrying plates.

So, returning to Figure 2, we see that the Poynting flux that flows predominantly between the two current systems (upward and downward) does not flow along the magnetic field lines but rather along the contours of constant electric potential. Specifically, the Poynting flux can focus in on the region where there are components of the electric field that are parallel to the magnetic field and that provide the principal power source for the auroral acceleration that occurs at those positions.

How large is this static current Poynting flux? With perpendicular electric fields (~0.5 V m^{-1}) and the perpendicular magnetic fields (200 nT) measured at low altitudes by the FAST mission as reported by *Carlson et al.* [1998], power density values of 100 ergs cm^{-2} appear easy to come by. So it is clear that the Alfvén wave Poynting flux by no means dominates over the Poynting flux for static fields and currents. However, we do not know the relative ranking of these two sources when it comes to efficiency of conversion from electromagnetic energy to particle energy. The Alfvén wave Poynting flux can certainly be an important contributor, consistent with the finding of *Keiling et al.* [2003]. Also, nothing in this discussion specifically demonstrates that the Alfvén wave Poynting flux cannot be one of the drivers, through some conversion process, of the static current and field configurations observed at lower latitudes. But we see that much more is needed than arguments that simply compare the quantity of power available from a possible power source with the quantity of power dissipation. We will return to this topic when we discuss auroral power generation at Jupiter.

1.3. Auroral Regions and Regimes at Earth

Several different auroral regimes are of interest (Figure 4) besides the discrete auroral component that we have been

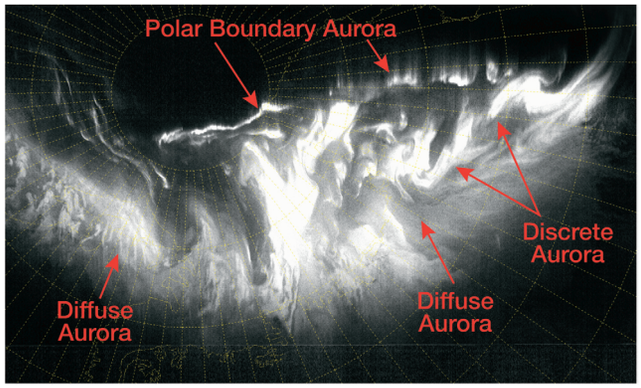

Figure 4. Key regions of the Earth's aurora. The diffuse aurora is identified by the spatial homogeneity of the emission and the smooth and unstructured nature of the spectra of the precipitating electrons. The discrete aurora is identified by the spatially structured character of the emissions and the structured nature of the spectra of the precipitating electron distributions, often showing peaked features indicative of acceleration along field lines. The polar boundary aurora is a discrete auroral feature that resides near the boundary between closed and open field lines. Image from the Defense Meteorological Satellite Program (DMSP).

discussing. While these auroral regimes are expected to have a certain latitudinal ordering, statistical distributions show that there is much overlap (Figure 5) [*Newell et al.*, 2009]. We have not yet mentioned the diffuse aurora that generally resides at the lowest latitudes (Figures 4 and 5a). Diffuse electron aurora, with emissions that are relatively spatially uniform and with unstructured precipitating electron spectra, are thought to result from the scattering of hot electrons that are trapped in the magnetic field of the distant magnetosphere into the magnetic loss cone (comprising those charged particles whose magnetic mirror points reside within the Earth's atmosphere or below). The scattering occurs as a result of strong interactions between the trapped particles and various kinds of plasma waves that reside within the trapped plasma populations. The wave modes thought to be responsible for the scattering are electron cyclotron harmonic waves and/or "chorus" whistler mode waves [*Horne et al.*, 2003; *Ni et al.*, 2008; *Meredith et al.*, 2009; *Su et al.*, 2010]. Interesting

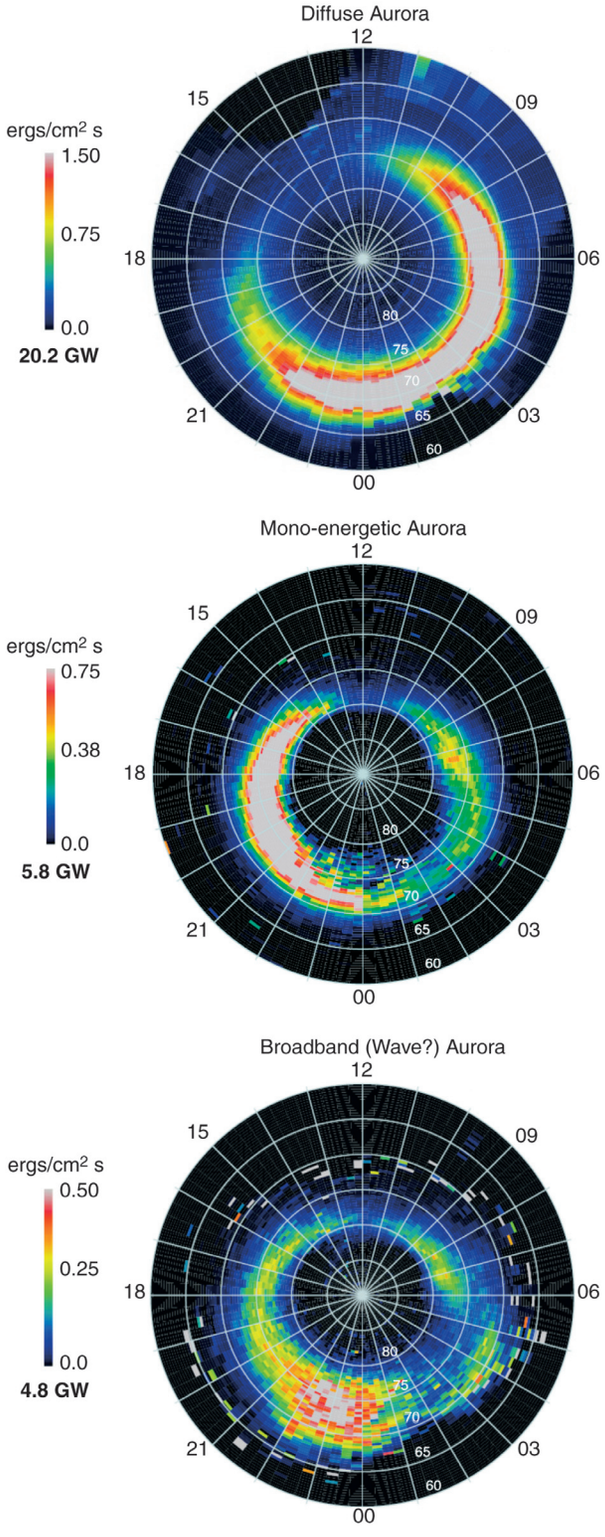

Figure 5. Statistical study of the different kinds of Earth aurora. Shown are binned and averaged particle energy depositions as determined from the particle spectrometers on the low-altitude polar DMSP spacecraft. The different kinds of energy depositions are determined and cataloged according to the characters of the shapes of the particle energy spectra. The cataloging and binning is automated using a neural network algorithm. The "GW" values shown below the color bars are the power in gigawatts of particle energy deposited as integrated over each entire image. From *Newell et al.* [2009].

dynamic features of the diffuse electron aurora are discussed by *Lessard* [this volume] and by *Li et al.* [this volume], and proton diffuse auroras are discussed by *Donovan et al.* [this volume]. Note that the overall energy carried into the diffuse electron auroral regions is larger than that provided by any other component (Figure 5), although the intensity is well below that provided by the discrete processes.

At midlatitudes (Figures 4 and 5b) are the so-called discrete auroral emissions that traditionally are thought to be synonymous with the monoenergetic auroral acceleration, which in turn is thought to be the result of the quasi-static current and field configurations discussed above in reference to Figure 2 [e.g., *Carlson et al.*, 1998]. With the quasi-static discrete auroral mechanisms, there are two different regions (Figure 2) that are of substantial interest: (1) the region of upward currents that engender downward accelerated electrons (and upward accelerated ions) and strong discrete auroral emissions, and (2) the region of downward currents that engender powerful upward accelerated electrons that are commonly detected near the equatorial regions of the magnetosphere. The upward accelerated electron distributions constitute a powerful tool for mapping auroral regions to the distant magnetosphere, as we shall see.

The aurora at higher latitudes (Figures 4 and 5c) is where the Alfvén wave processes [*Keiling et al.*, 2002; *Schriver et al.*, 2003; *Chaston et al.*, 2003], discussed in section 1.2, may contribute to the discrete auroral emissions. At the highest latitudes are the "polar boundary auroral emissions" (Figure 4) that may be driven by the Alfvén wave processes described here, but could also be a consequence of the quasi-steady electric currents associated with the open-closed boundary. This boundary is between lower-latitude closed magnetic field lines that have both of their ends connected to the ionosphere and the higher-latitude open magnetic field lines with one end connected to the ionosphere and the other end connected to interplanetary space. This auroral boundary is thought to be connected to distant regions where magnetic energies are converted to plasma and particle heating through "magnetic reconnection" [*Bunce*, this volume]. The reader will note that issues of which physical mechanisms are responsible for specific observed phenomenological features remain rich areas for research.

As a final note, in the history of the study of auroral emissions and features coming from terrestrial and other planetary systems, it has often been assumed that strong aurora occur predominantly near but inside the boundary between open and closed field lines. Figure 4 shows high-latitude auroral emissions (polar boundary aurora) that likely map close to that transition boundary. However, while there is present controversy surrounding the premise that transients within the boundary auroral regions provide a trigger for features occurring at lower latitudes [*Lyons et al.*, 2010; *Nishimura et al.*, 2010; *Lyons et al.*, this volume], it is clear that the strongest discrete emissions occur well equatorward of that transition region. Strong discrete auroral emissions during such geomagnetic disturbances, called magnetic storms and substorms, are thought to map to the vicinity of 9 to 12 R_E at Earth [e.g., *Akasofu et al.*, 2010, and references therein], while the reconnection sites that may or may not provide the stimulus for strong auroral breakups are thought to occur in the vicinity of 20 R_E and beyond [e.g., *Nagai et al.*, 2005]. The distances between 20 and 9 to 12 R_E certainly cannot be considered "near."

2. COMPARING PLANETARY AURORAL SYSTEMS

2.1. An Approach to Comparing Planetary Magnetospheres

In the discussions that follow, we compare electromagnetic parameters between several of the strongly magnetized planets using an "electrical circuit" approach, and more often than not, we compare the electric currents and electric fields of these respective systems. For the valid reasons mentioned below, it has become unfashionable in recent times to take this circuit approach and, specifically, to speak of electric fields and currents, following the publication of the now famous work by *Vasyliūnas* [2001] and also later discussions [e.g., *Vasyliūnas*, 2011, and references therein]. The values of the circuit approach are (1) it is easy to conceptualize the strong interactions between very different components of a complex system, for example, spanning regions that are controlled by kinetic factors and those dominated by magnetohydromagnetic factors and (2) the historical literature is presently dominated by such approaches, and any review such as this must incorporate them. The disadvantage of this approach is that it is valid only for quasi-static situations, by which we mean that the time scales for changes must be much slower than the Alfvén wave transit times for the region of consideration [*Vasyliūnas*, 2011]. We note that Alfvén transit times are also important for time-stationary configurations for systems that include, for example, the outer portions of Jupiter's huge magnetosphere, where the time for the transit of an Alfvén wave from the inner to the outer reaches of the system is a substantial fraction of Jupiter's rotation period. It is undoubtedly true that future advances in our understanding of planetary auroral phenomena will require such nonsteady approaches as those advocated by *Vasyliūnas* [2011].

So, despite the limitations mentioned above, the crude conceptual framework that we consider in this chapter is provided in Figure 6. Our purpose in showing this too simple figure is not to argue about or defend the particular way that we have connected up the different boxes, but to place

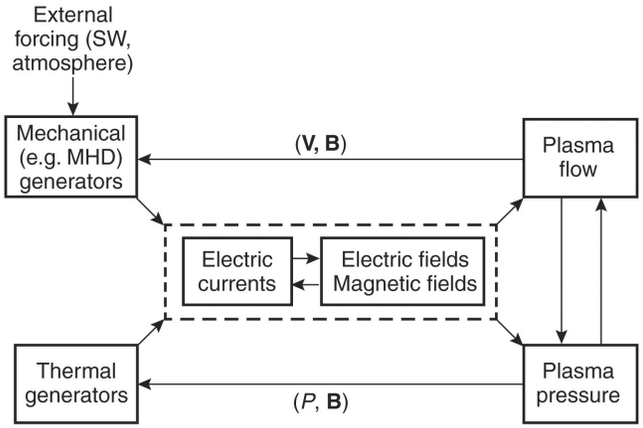

Figure 6. An electrical circuit framework for discussing differences between the electromagnetic environments and auroral systems of the strongly magnetized planetary systems. See text for a discussion of the deficiencies and criticisms of the electrical circuit approach. The purpose of this too-simple diagram is to place thermal (pressure) effects on a more equal footing with dynamical (flow) effects than has been evident in the literature at extraterrestrial magnetospheres.

thermal and dynamical effects (shown with the bottom and top feedback loops in the figure) on a more equal footing than has been evident in much of the literature at extraterrestrial magnetospheres.

2.2. Comparing Planetary Magnetospheres

Given that the auroras at some different planets have strong superficial similarities (Figure 1), it is of interest to understand how the corresponding magnetospheric systems are similar and how they are different. At the highest levels, there are several different conditions that seem to drive important differences between known planetary magnetospheric systems. Two of these conditions are (1) the relative strength of the plasma flows generated within the magnetosphere by the solar wind and by planetary rotation and (2) the presence or absence of a strong internal source of plasma.

With regard to the first of these conditions, the interaction between the fast-flowing solar wind and the magnetosphere, in the form of magnetic reconnection and flows driven inside but in the vicinity of the outer boundary of the magnetosphere, generates electrical currents on the boundary which close in various places within the magnetosphere and ionosphere. Those interior currents and their divergences generate electric fields and plasma motions deep within the interior of the magnetosphere. Empirically, the interior electric field is a fraction of the solar wind electric field ($\mathbf{E_{SW}} = \mathbf{V_{SW}} \times \mathbf{B_{SW}}/c$), with magnitude E_{SW}, and traditionally and heuristically, researchers have spoken of an electric field $\mathbf{E_p}$ that "penetrates" across magnetospheric boundaries, even while that characterization is highly imprecise. Traditionally, the strength and direction of the externally driven electric field within the interior of the magnetosphere is represented as:

$$\mathbf{E_p} \sim f \cdot \mathbf{E_{sw}} = \overrightarrow{\nabla}(f \cdot \mathbf{E_{sw}} \cdot R \cdot \sin[LT]), \quad (1)$$

where f is the empirically estimated fraction of the external (to the magnetosphere) solar wind electric field that ends up inside the magnetosphere (at Earth $f \sim 0.1$), $\mathbf{V_{sw}}$ is the solar wind velocity (~400 km s^{-1}, assumed to be uniform), $\mathbf{B_{sw}}$ is the magnetic field within the solar wind (~8 nT at Earth, assumed to be uniform), and c is the speed of light. The right-hand portion of equation (1) reformulates the interior electric field in the form of the gradient of a potential. Here Φ_{sw} is the electric potential whose gradient yields a uniform cross-magnetosphere electric field, R is the geocentric radial distance, and LT is the local time expressed in radians. This solar wind–generated electric field is traditionally to be compared with the rotational electric field. When the conducting ionosphere, frictionally dragged by the rotating upper atmosphere, rotates within the planet's magnetic field, a $\mathbf{V} \times \mathbf{B}/c$ electric field is generated within the ionosphere. Under the ideal condition that the magnetic field lines (when populated with plasmas) act as nearly perfect conductors, and when opposing equatorial forces and accelerations are small, the equatorial rotational electric field becomes:

$$\overrightarrow{E}_{\text{rot}} = (\overrightarrow{\Omega} \times \overrightarrow{R}) \times \overrightarrow{B}/c = \overrightarrow{\nabla}(\Phi_{\text{rot}}) = \overrightarrow{\nabla}\left(\frac{\mathbf{\Omega} \cdot B_O}{c \cdot R}\right), \quad (2)$$

where $\mathbf{\Omega}$ is the planetary rotation vector aligned with the planet's spin axis and Φ_{rot} is the equatorial electric potential that results when the planetary magnetic field B is a dipolar configuration with a normalization strength constant B_o (as in equatorial $B = B_o/R^3$) and with the dipole moment aligned with $\mathbf{\Omega}$. Combining rotational and solar wind electric potentials yields (see various approaches and discussions by *Axford and Hines* [1961], *Nishida* [1966], *Brice* [1967], *Kavanagh et al.* [1968], *Chen* [1970], *Brice and Ioannidis* [1970], and *Vasyliūnas* [1975]):

$$\Phi_{\text{tot}} = \frac{\mathbf{\Omega} \cdot B_O}{c \cdot R} + f \cdot \mathbf{E_{sw}} \cdot R \cdot \sin(LT), \quad (3)$$

which, when plotted for contours of constant Φ_{tot}, evaluated using the parameters in Table 1, yields the patterns like those shown in Figure 7 (T. W. Hill contribution to the review by *Mauk et al.* [2009]) for Earth, Jupiter, and Saturn. These diagrams, representing the patterns of flow for low-energy plasmas and particles (representing the $\mathbf{E} \times \mathbf{B}/c$ drift) [*Parks*, 1991], ignore the deviations near the magnetosphere boundaries and

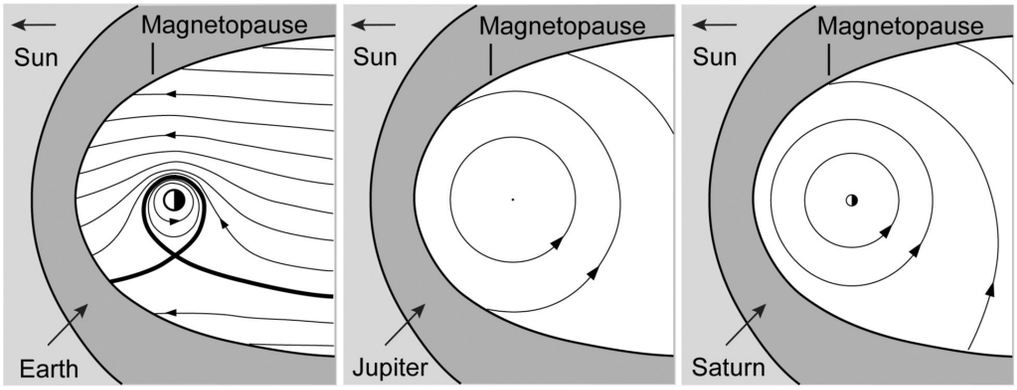

Figure 7. Simple model prediction of equatorial cold plasma flow patterns within the magnetospheres of the Earth, Jupiter, and Saturn. Deviations close to the magnetopause and within the deep magnetotail are not modeled here. Figure 7 provided by T. W. Hill for the review of *Mauk et al.* [2009 , Figure 11.15] of Saturn's magnetospheric processes. Reprinted with kind permission from Springer Science + Business Media.

within the deep tail. In consideration of the criticisms of the unfashionable use of electric field representations in section 2.1, we note that T. W. Hill (again in the review by *Mauk et al.* [2009]) derives these flow patterns from a consideration of the summation of flows rather than with the historical approach of using electric fields. The plots in Figure 7 indicate that the Earth's magnetosphere is powered predominantly by the solar wind and that the magnetospheres of Jupiter and Saturn are powered predominantly by rotation. At Saturn, the role of the solar wind is controversial and may be more important than is indicated by Figure 7 for driving auroral phenomena [*Cowley et al.*, 2004; *Bunce et al.*, 2008; *Bunce*, this volume].

Another factor that seems to be critical in understanding similarities and differences between planetary magnetospheres and their auroral systems is the presence or absence of a strong internal source of plasma, such as the volcanic action of Jupiter's satellite Io (at 5.9 R_J) and the venting activities of Saturn's satellite Enceladus (at ~4.0 R_S). Some of the emitted gases are ionized and energized by being picked up by the rapidly corotating plasma. Because these plasmas are generated near the rapidly rotating planet, and therefore near the peak of a centrifugal potential hill that falls with increasing radial distance, further energization occurs as the plasmas move outward. Some of the energy associated with the internal generation and transport of these new plasmas is tapped to drive various magnetospheric processes, including dramatic auroral displays. The generation, heating, transport, and loss of the gases and plasmas at Jupiter and Saturn remain poorly understood (see review by *Bagenal and Delamere* [2011]).

Table 2 categorizes all of the magnetized planets of the solar system with respect to our two conditions: (1) solar wind influence and (2) the presence or absence of a strong internal source of plasma. Table 2 was created to provide evidence for the hypothesis that these two conditions are deterministic with regard to the presence or absence of dynamic injection-like phenomena within the respective magnetospheres. Injections are sudden planetward plasma transport events that occur over a limited range of longitudes. At Earth, they are associated with geomagnetic disturbance events called substorms. While Table 2 does seem to order the planets with respect to dynamics (injection-like phenomena occur in magnetospheres that are either powered by the solar wind or by centrifugal energies of strong, internally generated plasma), an outstanding mystery with regard to the occurrence of strong auroral phenomena is Uranus. Uranus was powered by the solar wind because of the Sun-aligned spin axis at the time of the Voyager 2 encounter [*Selesnick and McNutt*, 1987]; this condition is not generally true of Uranus, just true at the time of the Voyager 2 encounter. That magnetospheric phenomena at Uranus were

Table 2. Sorting the Planets According to Solar Wind Influence and Internal Plasma Sources

Planet	Injections?	Solar Wind Dominance?	Strong Internal Source?
Mercury	yes	yes	no
Earth	yes	yes	maybe: atmosphere
Jupiter	yes	no (rotation)	yes (Io)
Saturn	yes	no (rotation with sw triggering?)	yes (Enceladus)
Uranus	yes	yes (peculiar orientation)	no
Neptune	no (none observed)	no	no: Triton is "middle" source

driven by the solar wind during the Voyager 2 encounter is supported by observations of solar wind–driven flow configurations [*Selesnick and McNutt*, 1987], strong dynamic injection phenomena [*Mauk et al.*, 1987; *Belcher et al.*, 1991], whistler/chorus plasma wave emissions that were more intense than Voyager observed at any of the other planets [*Kurth and Gurnett*, 1991], and radiation belt electrons as intense as those observed during supermagnetic storms at Earth [*Mauk and Fox*, 2010]. Yet, auroral emissions with the high powers and ordered (ringed) structures of the sort observed at Earth, Jupiter, and Saturn were not observed at Uranus) [*Herbert and Sandel*, 1994; *Herbert*, 2009] (Figure 1 compare power levels in Table 1). So there are factors that control the occurrence or absence of intense auroral phenomena; factors that have not yet been identified. Possibly, the constantly changing geometry associated with the large magnetic axis tilt (Table 1) and planetary rotation, given an interplanetary magnetic field not aligned with the planet-Sun line, has a role to play.

On the other hand, at Neptune, because the rotational forcing is much larger than the solar wind forcing despite the period modulations, given the large tilt of the magnetic axis [*Selesnick*, 1990], and also because of the absence of a strong internal source of plasma, the aurora is expected to be relatively inactive, and indeed, its auroral emissions are far below those observed at other planets, even lower than those observed at Uranus (Table 1) [*Bishop et al.*, 1995].

A referee to this chapter thoughtfully suggested a third global-controlling parameter for comparing magnetospheres: the amount of solar wind flow energy that impinges on the cross section of the magnetosphere. With this parameter, the referee argues, the relative weakness of Uranus' aurora relative to those of the other active planets is understandable. A puzzle is that other aspects of Uranus' magnetosphere, discussed in the previous paragraph (radiation belt intensities, whistler mode activity), are as energetic as those of the Earth in its most active state.

The auroral emissions that do occur at Uranus and Neptune are thought to be most closely associated with the diffuse aurora at Earth (section 1.3) in that they have been interpreted in the context of scattering of magnetospheric particles onto the atmosphere without the additional energization that accompanies the other auroral processes [*Herbert and Sandel*, 1994; *Bishop et al.*, 1995]. For the rest of this chapter, we focus most of our attentions on the discrete auroral processes at Earth, Jupiter, and Saturn.

2.3. Comparing Auroral Current Systems

Here we describe the differences between auroral current systems driven by the solar wind (Earth), and those driven predominantly by rotation (Jupiter and perhaps Saturn). The relationship between global current systems and magnetospheric regions and dynamics is addressed in section 5 of this volume.

The Earth's aurora current system is driven by strong coupling between the flowing magnetized solar wind and the magnetosphere. Aspects of those current systems are shown in Figure 8 [*Cowley*, 2000; *Stern*, 1984]. On the dayside magnetopause (the boundary between the interplanetary medium and the Earth's magnetosphere), magnetic reconnection (a process that connects interplanetary magnetic field lines together with the Earth-connected field lines and converts magnetic energy to plasma heating and flow) is thought to allow the motional ($\mathbf{V} \times \mathbf{B}/c$) electric field of the solar wind to effectively penetrate inside the magnetosphere. Thus, momentum from the solar wind is coupled to the magnetosphere, drives a two-cell flow pattern within the ionosphere (Figure 8b), and maintains a system of upgoing and downgoing magnetic field-aligned electric currents called region 1 and region 2 (Figures 8a and 8b). How the region 1 system of current sheets, thought to close in the vicinity of the magnetopause on the dayside (Figure 8a), connects across the antisunward, comet-like magnetic tail is uncertain, but one solution is suggested in Figure 8c [*Stern*, 1984]. A dynamic version of the diversion of the cross-tail current into the ionosphere shown with this shunting process is also associated with dynamical events within the magnetosphere giving rise to auroral breakups associated with geomagnetic substorms. The region 2 currents are thought to be closed by the hot ion populations (ring current populations) trapped within the Earth's middle and inner magnetosphere (Figure 8a). So within any one meridional plane, there is a system of upgoing and downgoing electric currents (regions 1 and 2) that mimics the pair of currents sketched in Figure 2. However, during active conditions, the auroral regions are highly structured (Figure 4) [e.g., *Gorney*, 1991], and there are often multiple pairs of upgoing and downgoing currents [*Elphic et al.*, 1998]. How such structuring comes about is a mystery. Note that statistically (Figure 5) the occurrence of strong discrete aurora (and indeed the Alfvénic aurora as well) maximizes in the premidnight region, consistent with the current-flow sense of the region 1 currents (upward currents associated with downward electron acceleration).

Jupiter's auroral current system is driven by rotational energy combined with the production and outward transport of iogenic plasma [*Hill*, 2001; *Cowley and Bunce*, 2001]. These rotationally symmetric currents close through the ionosphere to generate a large-scale meridional current system like that illustrated in Figure 9a [*Hill*, 1979; *Vasyliūnas*, 1983]. A consequence of the current closure is that the rotation of the ionosphere is coupled to the rotation of the equatorial plasmas, and the equatorial plasmas are

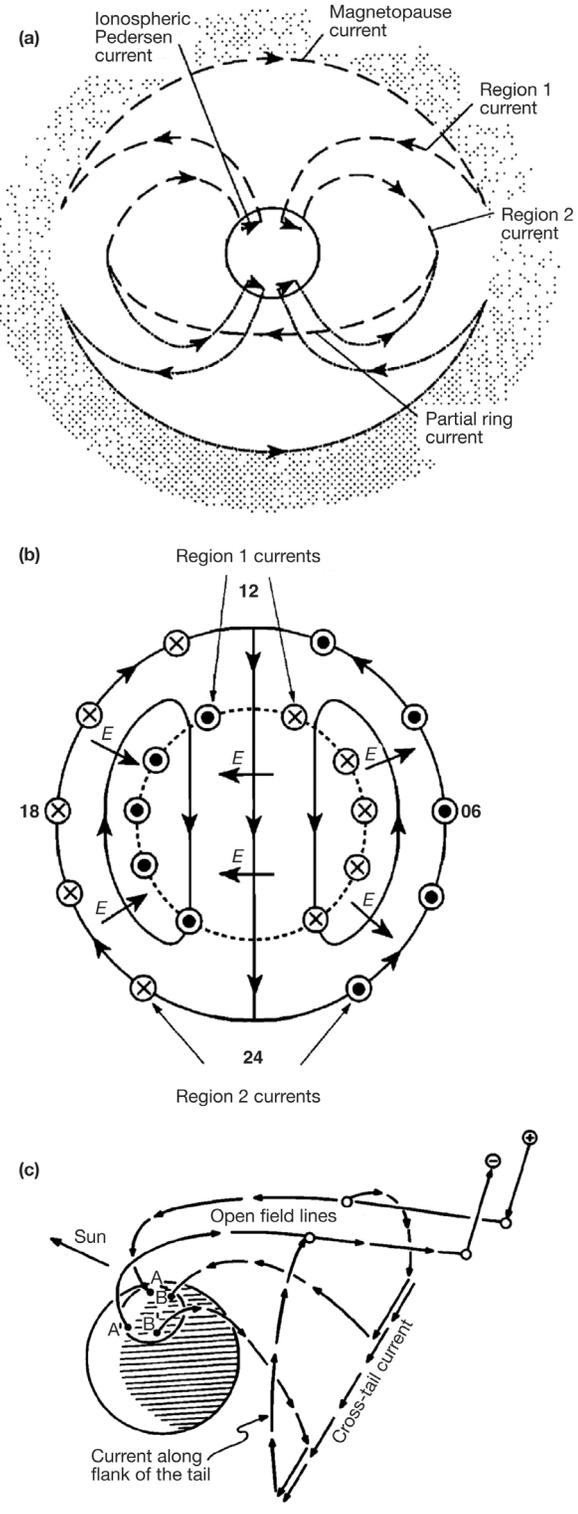

accelerated to a substantial fraction of the rigid rotation speed [*Hill*, 1979]. Rotational speeds as a function of radial distance stay at higher levels than the *Hill* [1979] theory would suggest (taking into account ionized mass outflow from the regions of the moon Io), indicating that modifications engendered by magnetic field-aligned electric fields and auroral precipitation (particle impacts on the ionosphere which increases conductivity) are substantial [e.g., *Ray et al.*, 2010; *Ray and Ergun*, this volume].

Just as we find at Earth, observations at Jupiter of particle acceleration features (section 2.5) indicate that the auroral currents are much more structured than suggested by Figure 9a, with multiple pairs of upward and downward currents occurring [*Mauk and Saur*, 2007]. A notional current profile as a function of magnetospheric L at some unspecified, nonequatorial latitude is sketched in Figure 8b. *Saur et al.* [2003] have suggested that the structuring is so pervasive on multiple scales that turbulent processes may be the prime energy conversion mechanism for the generation of Jupiter's aurora. This notion is supported by the power densities and spatial distribution (matching the mapped auroral distribution) of the magnetic turbulent spectrum (see Figure 10). More specifically, *Saur et al.* [2003] argue that there is a sufficient source of energy within the magnetic turbulence to power Jupiter's main aurora. We focus on this suggestion because it is highly reminiscent of the "Alfvénic aurora" discussion in section 1.2 about the Earth's aurora. Just as has been done in the case of the Earth, the argument is supported principally on the basis of energy source (rather than a specific mechanism for energy dissipation) and on the magnetic mapping of structures from the magnetosphere to the auroral dissipation regions. Not only does the region of turbulence at Jupiter map well to the regions of auroral emissions, but the energies available for dissipation from that turbulence are sufficient to provide all of the energy needed to power the aurora. The role of turbulent waves in transporting energy from the magnetosphere to the auroral regions, and in possibly helping to drive the auroral current system, is a ripe area for research on both the Earth and Jupiter and likely on other systems as well.

Figure 8. Schematics of the solar wind–driven auroral current system at Earth. (a) A view toward the Sun with the inner boundary of the shaded region representing the outer boundary of the magnetosphere. (b) A view of the Earth's Northern Hemisphere ionosphere. The crosses and dots represent magnetic field-aligned currents flowing into and out of the ionosphere. Figures 8a and 8b are from *Cowley* [2000]. (c) The antisunward, comet-like magnetic tail of Earth's magnetosphere extends to the right. Figure 8c is from *Stern* [1984].

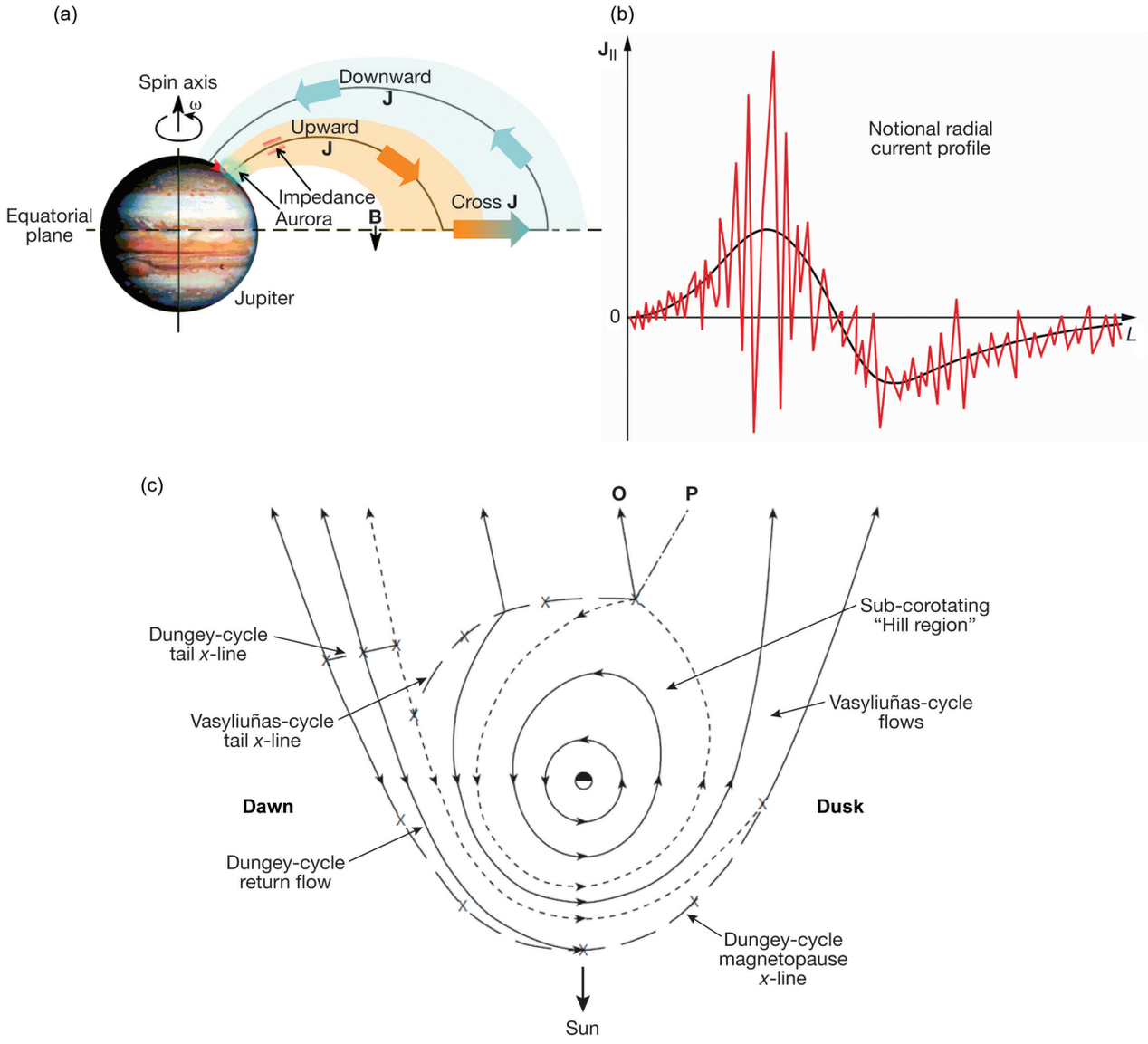

Figure 9. Auroral current systems at Jupiter. (a) Currents within a meridional plane. The structures shown are azimuthally symmetric. (b) A notional radial cut through the currents in Figure 9a at midlatitudes. Figures 9a and 9b are from *Mauk and Saur* [2007]. (c) A theoretical equatorial flow pattern at Jupiter [from *Cowley et al.*, 2003; see *Badman and Cowley*, 2007].

Continuing with Jupiter, Figure 9c [*Badman and Cowley*, 2007] shows theoretical flow patterns both within the inner regions discussed above and also in the more distant regions where solar wind effects may have a role to play, particularly within the magnetic tail. A key feature is the tail reconnection line (labeled Vasyliūnas cycle in Figure 9c) [*Vasyliūnas*, 1983] where field lines populated with dense plasmas from Io disconnect and flow down the tail. The figure shows a second, distinct reconnection line (labeled Dungey cycle in Figure 9c) that accommodates the return flow associated with solar wind–driven motions. It is clear that at Jupiter, a very small portion of the large-scale pattern is driven by solar wind forcing, but the current debate is whether there is a distinct channel (labeled Dungey cycle return flow in the diagram of Figure 9c), whether open flux is closed and returned mixed-in with the Vasyliūnas cycle [*Badman and Cowley*, 2007], or whether the solar wind actions are confined to a viscous boundary layer [*McComas and Bagenal*, 2007; *Delamere and Bagenal*, 2010]. *Delamere* [this volume] addresses Jovian auroral signatures associated with the solar wind interaction at Jupiter.

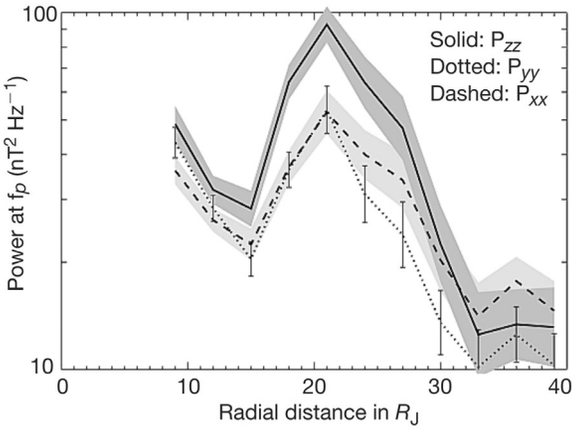

Figure 10. Distribution of the total measured magnetic turbulence power within the equatorial regions of Jupiter' magnetosphere both parallel (*z*, solid line) and perpendicular (*x* and *y*, dashed and dotted) to the local magnetic field direction calculated from magnetic fluctuations on the basis of weak turbulence theory involving Alfvén waves. *Saur et al.* [2003] propose that such turbulence may represent a key power source for Jupiter's aurora.

At Saturn, it is argued [*Bunce et al.*, 2008; *Bunce*, this volume] that the solar wind forcing has a more prominent role in the outer magnetosphere than at Jupiter. It is further argued that rotational forcing is insufficient to generate intense aurora at Saturn and that magnetic reconnection within the deep magnetotail is moderated by the solar wind and is the driver of intense auroral emissions and dynamics at Saturn. Various positions on the role of the solar wind in generating Saturn's aurora are discussed broadly in the review by *Kurth et al.* [2009], and we will not summarize them here. We show in the discussions that follow, however, some examples of auroral phenomena that map to the deep interior of Saturn's magnetosphere, contrary to the models referenced above, which model Saturn's aurora as powered by tail reconnection and mapping to positions close to the site of the reconnection. It is now clear that Saturn's auroral configuration and dynamics are more complicated than any one model can accommodate. This finding should be no surprise, since the same thing can be said for the Earth. At Earth, many observers believe that magnetic reconnection driven by the solar wind within the magnetic tail is a prime mover of auroral energetics and dynamics, but it is clear that the most intense auroral phenomena often occur well equatorward of the reconnection site (Figure 4). Unlike at Earth, at Saturn, there is still the open question of what the ultimate source of power is for the most intense aurora. Is it rotational energy that the solar wind helps trigger and moderate, or is it solar wind energy input itself?

2.4. Current Closure

An important aspect of the differences between the global currents of different auroral systems is how the currents close within the distant equatorial magnetosphere. In discussing such current closures, we again point out differences and similarities between systems driven by the solar wind and systems driven by rotation.

Using the guiding center approach in analyzing the motions of particles within a magnetic field, the total current density $\mathbf{J}_\perp$ perpendicular to the magnetic field can be written as [*Parks*, 1991]:

$$\mathbf{J}_\perp = \frac{\mathbf{b}}{B} \times \nabla_\perp (P_\perp) + (P_\parallel - P_\perp) \frac{\mathbf{b} \times (\mathbf{b} \cdot \nabla)\mathbf{b}}{B} + (m \cdot n) \frac{\mathbf{b}}{B} \times \frac{\mathrm{d}\mathbf{V}}{\mathrm{d}t}, \quad (4)$$

where, $\mathbf{b}$ is the unit magnetic field vector, B is magnetic field strength, P is the particle pressure, the symbols $\perp$ and "$\parallel$" indicate parameters measured perpendicular and parallel to the magnetic field direction, m is the average mass per ion, n is the number density, $m \cdot n$ is the mass density, and $\mathbf{V}$ is the flow velocity. Note that the $\mathrm{d}\mathbf{V}/\mathrm{d}t$ operation is a total derivative that includes both the explicit time dependence and the time-stationary convective contribution [$\mathrm{d}\mathbf{V}/\mathrm{d}t = \partial\mathbf{V}/\partial t + (\mathbf{V} \cdot \nabla)\mathbf{V}$]. The first of the three terms of equation (4) is the diamagnetic current driven by gradients in the hot plasma pressure. The second term is what remains of the currents from guiding center drifts that arise from the presence of gradients and curvatures within the magnetic field configuration after partial cancellation from terms associated with magnetization (contributions from $\nabla \times \mathbf{M}$, where $\mathbf{M}$ is the magnetic moment per volume of the plasma medium; the diamagnetic current is one of the magnetization current contributions). The third term represents currents associated with the acceleration of the plasma population. Notice that for an isotropic distribution ($P_\parallel = P_\perp$), the second term is zero, leaving only the diamagnetic and acceleration terms. Equation (4) shows only currents perpendicular to the magnetic field direction, but it is, of course, the divergence of the perpendicular currents ($\nabla \cdot \mathbf{J}_\perp$) that yields the parallel currents that close through the auroral ionosphere.

For the Earth's magnetosphere, region 2 currents are thought to be closed by the diamagnetic (first term of equation (4)) current closure term (Figure 8a) [see *Cowley*, 2000], with field-aligned currents generated by divergences resulting from transport-engendered asymmetries. The region 1 currents on the dayside are thought to be closed by the acceleration term (third term of equation (4)) associated with the sheared solar wind flow in the vicinity of the magnetopause boundary between the Earth's magnetic field and the solar wind on the dayside. However, a great uncertainty is

associated with the region 1 currents and the transient substorm currents that cross the magnetic tail regions. In the vicinity of the boundary between open and closed field lines within the magnetotail, a region thought to be regulated by magnetic reconnection, flow gradients engendered by the reconnection process may close the currents associated with the boundary aurora (Figure 4). Planetward and equatorward of that boundary, some models tap into the deceleration of the reconnection-generated earthward flows, combined with the adiabatic heating of compression as the plasmas flow earthward, to drive auroral currents [e.g., *Zhang et al.*, 2007; *Keiling et al.*, 2009; *Pu et al.*, 2010]. The relative roles of the acceleration term and the diamagnetic term in this process are uncertain. Determining the mechanism of current closure at the base of the magnetotail for strong dynamical auroral emission processes is one of the outstanding questions surrounding auroral physics at Earth.

For the nonterrestrial planets like Jupiter and Saturn, it is useful to separate the rotation term from the acceleration term. Specifically, under the assumption that there are no explicit time dependencies, one may jump into a rotational frame of reference using the standard textbook [e.g., *Fowles and Cassidy*, 1993] decomposition of the d**V**/d*t* term to yield:

$$\mathbf{J}_{\perp} = \frac{\mathbf{b}}{B} \times \nabla_{\perp}(P_{\perp}) + (P_{\parallel} - P_{\perp}) \frac{\mathbf{b} \times (\mathbf{b} \cdot \nabla)\mathbf{b}}{B} + (m \cdot n) \frac{\mathbf{b}}{B} \times [\boldsymbol{\Omega}_{pl} x (\boldsymbol{\Omega}_{pl} \times \mathbf{R})] + (m \cdot n) \frac{\mathbf{b}}{B} \times (2 \cdot \boldsymbol{\Omega}_{pl} \times \mathbf{U}_{\mathrm{rad}}), \quad (5)$$

where $\boldsymbol{\Omega}_{pl}$ is the rotational rate vector of the plasmas around the planet's spin axis (not necessarily the rotational rate vector of the planet itself), and $\mathbf{U}_{\mathrm{rad}}$ is the radial flow velocity of the plasma within that rotating frame of reference. Note that one may transform into the rotational frame that rotates rigidly with the planet, but for that formulation, there is an additional acceleration term associated with the deviation from rigid corotation. The transformation used here in equation (5) has the disadvantage of being useful only at one particular radial position with a plasma rotation rate of $\boldsymbol{\Omega}_{pl}$ (see a more complete treatment by *Vasyliūnas* [1983]).

The last two terms of equation (5) make sense if one considers the guiding center response of gyrating charged particles. In the presence of an electric field (**E**), plasmas flow with the well-known drift velocity: $c\ \mathbf{E} \times \mathbf{B}/B^2$. For an externally applied force (**F**) that acts only on mass rather than on charge, the drift velocity is $c \cdot m \cdot \mathbf{F} \times \mathbf{B}/(qB^2)$, where q is charge and m is mass, and where **F** is assumed to have the units force mass^{-1}. While the electric current associated with the **E** × **B** drift is zero, the electric current for the mass-dependent **F** × **B** drift is $(n \cdot m) \cdot \mathbf{F} \times \mathbf{B}/B^2$. With this understanding, we see that the third term of equation (5) is the **F** × **B** current associated with the centrifugal force (negative of the centripetal acceleration) and the fourth term is the **F** × **B** current associated with the Coriolis force due to outward flows of plasma that are continually generated by Io at Jupiter or Enceladus at Saturn.

For the conventional view of Jupiter's middle magnetosphere, which focuses on flow structure and dynamics [*Vasyliūnas*, 1983], it is the third term of equation (5) that provides the azimuthal currents that distort the magnetic field configuration away from the dipolar magnetic configuration toward the extended magnetodisc configuration. However, the diamagnetic currents are known to contribute substantially [*Mauk and Krimigis*, 1987; *Paranicas et al.*, 1991], and beyond 20 R_J, it has been found that the second term of equation (5), the so-called anisotropy term, has perhaps a dominant role [*Mauk and Krimigis*, 1987; *Paranicas et al.*, 1991; *Frank and Paterson*, 2004]. For the closure of the auroral current depicted in Figure 9a, it is the fourth term, the Coriolis term, that provides the radial, near-equatorial closure currents, to the extent that the flow configuration is thought to drive the auroral processes.

Historically, magnetospheric current closure associated with outer planet auroral current systems has been examined from the perspective of flow dynamic mechanisms [*Hill*, 2001; *Cowley and Bunce*, 2001; *Cowley et al.*, 2004; *Bunce et al.*, 2008], both flow dynamics associated with rotation and those associated with magnetic reconnection processes deep in the magnetic tail. It is thought that current closure by pressure-driven diamagnetic currents plays at least a minor role for Jupiter's aurora in providing, for example, the current closure for lower-latitude auroral patches equatorward of the main auroral ring (Figures 11c and 11d) associated with dynamic injection phenomena within the middle to inner magnetosphere [*Mauk et al.*, 2002b]. At Earth, such near-planet hot plasma injections generate magnetic field-aligned discharges, again, presumably associated with pressure-driven currents (Figures 11a and 11b) [*Mauk and Meng*, 1991]. The configuration (Figures 11b and 11d) of upgoing currents coming from one azimuthal boundary of the equatorial plasma cloud, and the downgoing currents coming from the other azimuthal boundary, comes naturally from the perpendicular diamagnetic current's scaling with the term $\nabla P/B$ (equation (5)). Along the contours of constant pressure (P), it is along the azimuthal boundaries of the injected clouds where $\nabla P/B$ diverges because of the variation of B, giving rise to the field-aligned currents. At Saturn, pressure-driven current contributions may be even larger. Specifically, *Mitchell et al.* [2009a] showed that a major auroral breakup-like display (Figure 12) was strongly correlated in time and space with a major middle-magnetosphere ion injection event centered near 13 R_S and revealed by

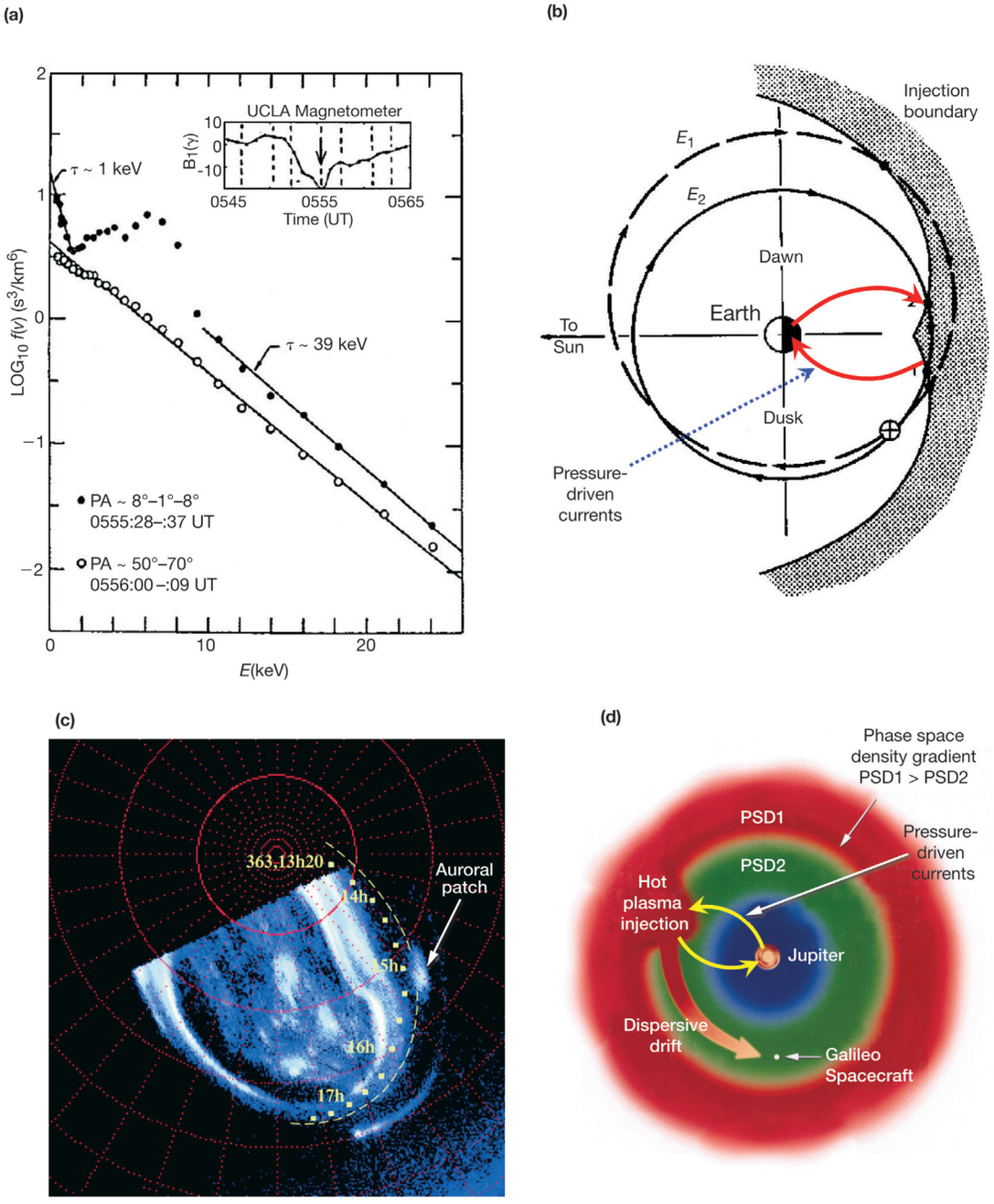

Figure 11. Magnetic field-aligned electrical beaming and magnetic field perturbations (a) associated with a hot plasma injection within the Earth's middle (geosynchronous) magnetosphere [*McIlwain*, 1975], thought to be associated with aurora emissions as diagnosed with auroral X-rays [*Mauk and Meng*, 1991]. These beams are interpreted here (b) as being associated with pressure-gradient-driven closure currents associated with the spatial configuration of the injected distributions. (c) Transient aurora at Jupiter, also associated with hot plasma injections [from *Mauk et al.*, 2002b] may also (d) be associated with hot plasma pressure-gradient current closure.

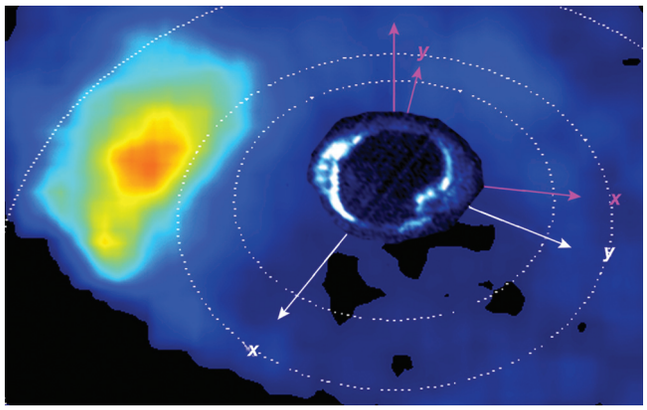

Figure 12. This is one frame of a movie that shows the correlation of the dynamics of a hot ion population (high-pressure region) as imaged with ~50 keV energetic neutral atoms (ENA) at Saturn by the Cassini magnetospheric imaging instrument, and the dynamics of a bright auroral storm occurring in Saturn's polar atmosphere as simultaneously imaged with the Cassini UVIS. The auroral image has been artificially inserted into the middle of the ENA image. The entire movie shows the simultaneous brightening of the ENA and UV emissions, centered about 45° anticlockwise from midnight and then the correlated rotation of both structures around dawn and into the dayside regions. The Sun is along the *x* axis shown in the figure. The ENA bright region is centered near ~13 R_S (between the dotted circle of the moon Rhea's orbit near 8.7 R_S and the dotted circle of the moon Titan's orbit near 20.3 R_S). Reprinted from *Mitchell et al.* [2009a], copyright 2009, with permission from Elsevier.

energetic neutral atom images, as both the ion injection feature and the auroral breakup feature rotated over several hours from the postmidnight regions into the dayside regions (Figure 12). On the basis of these features, a natural hypothesis is that pressure gradients are responsible for the current closure for the imaged auroral configurations for this event.

The source of the substantial populations of energetic particles is a major issue at Jupiter and Saturn, and the role of pressure-driven currents within the nonterrestrial planet auroral current systems is one of the great unanswered questions. It is significant that thermal energies dominate over the kinetic energy of flow velocities throughout the regions of both Jupiter's and Saturn's magnetospheres that connect to their aurora (Figure 13) [*Bagenal and Delamere*, 2011].

2.5. Particle Acceleration

2.5.1. Electron Acceleration. For the static auroral current systems, there are two regions of interest with regard to particle acceleration processes (Figure 2). The upward current region generates downward accelerated electrons, which excite the intense discrete auroral emissions [e.g., *Carlson et al.*, 1998]. These coherent distributions, often with monoenergetic peaks at ~1 keV to sometimes 30 keV energies at Earth, have not been observed within nonterrestrial planets because space probes have yet to visit regions with sufficiently low altitude and high latitude. Visiting such regions at Jupiter is a principal goal of the Juno mission, with Jupiter orbit insertion in 2016. Importantly, what has been observed on nonterrestrial planets are the upward accelerated electron distributions associated with the downward current regions [*Carlson et al.*, 1998; *Ergun et al.*, 1998]. These distributions have broad energy distributions (without a sharp peak in the energy spectra) and are narrowly confined to the magnetic field direction. Significantly, these upward accelerated electron distributions are observed in the near-equatorial regions and provide a powerful technique for mapping discrete auroral processes. They have been observed at Earth, Jupiter, and Saturn, and in the vicinity

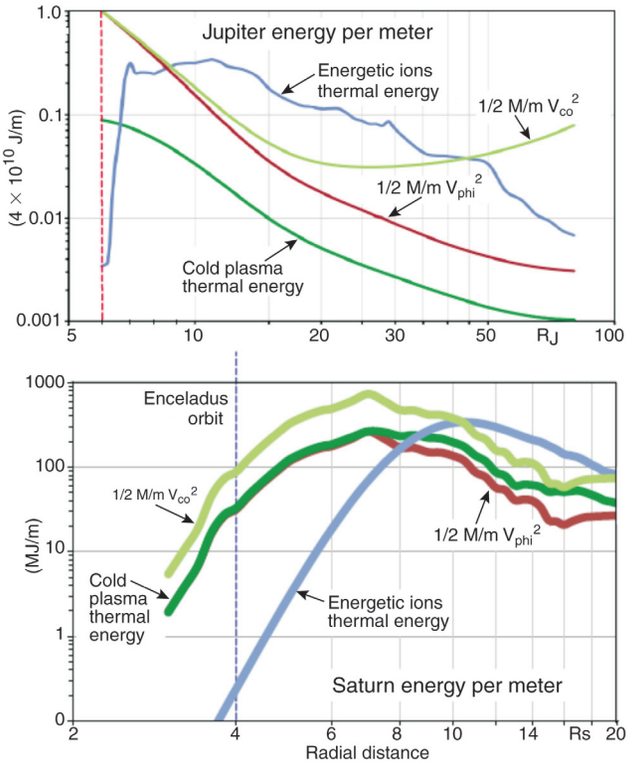

Figure 13. Energy profiles for (top) Jupiter and (bottom) Saturn where the energy density is summed over cylindrical annuli of width 1 m, and *M*/m is the total mass of plasma per cylindrical meter. The kinetic energy is shown for both rigid corotation and for observed $\mathbf{V}_{phi}$ profiles. The significance of this figure is that it shows that thermal energy densities are either comparable to, or dominate over, flow energy densities within the regions that map magnetically to the most intense auroral emission regions. From *Bagenal and Delamere* [2011].

of several of the satellites of these systems (Figure 14). They are interpreted in each environment as being associated with auroral acceleration [*Klumpar et al.*, 1988; *Carlson et al.*, 1998; *Williams et al.*, 1996; *Mauk et al.*, 2001; *Frank and Paterson*, 2002; *Mauk and Saur*, 2007; *Saur et al.*, 2006]. The mechanism of upward acceleration is thought to be stochastic acceleration through interactions with a multiplicity of small-scale electrostatic structures [*Ergun et al.*, 1998]. It is unknown whether or not this process is driven in the distant magnetosphere by the Alfvénic auroral generator discussed in section 1.2, the generator of quasistationary auroral currents or some other process.

At Earth (Figure 14a), the equatorial beams were observed by *Klumpar et al.* [1988] at ~9 R_E and were attributed to the consequences of downward accelerated electron beams. *Carlson et al.* [1998] reinterpreted these beams, on the basis

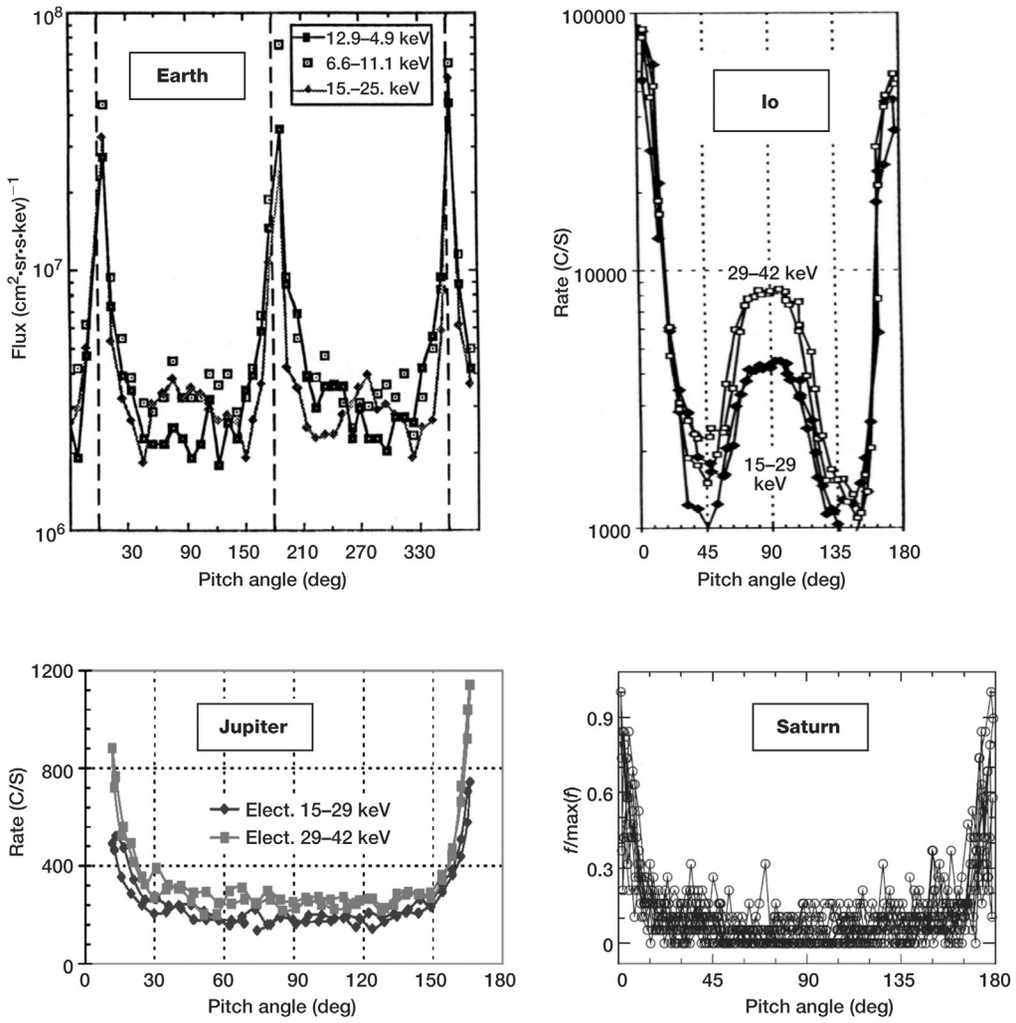

Figure 14. Equatorial magnetic field-aligned electron beams observed at Earth, Jupiter, Saturn, and in the vicinity of Jupiter's satellite Io. All have been associated with upward auroral electron acceleration by *Carlson et al.* [1998] (Earth panel from *Klumpar et al.* [1988]), at Jupiter by *Mauk and Saur* [2007], at Saturn by *Saur et al.* [2006] and at lo by *Williams et al.* [1996] and *Mauk et al.* [2001]. Pitch angle is the angle between the particle velocity vector and the magnetic field vector. The reader should exercise care, since the top two plots have logarithmic *y* axes, whereas the bottom plots have linear *y* axes. Also, the Earth plot shows a complete spacecraft spin, and the angles between 180° and 360° represent a second sampling of true pitch angles between 180° and 0°. Only the distribution observed near Jupiter's moon Io has a trapped population with pitch angle near 90°, presumably resulting from the localized magnetic field minimum detected very close to the moon.

of discoveries made with the FAST mission, as being the equatorial manifestation of the upward accelerated electron beams associated with the downward leg of the auroral electric currents (Figure 2). At Jupiter (Figure 14c), equatorial electron beams have been observed sporadically throughout the broad regions of downward currents in the global auroral current system (Figure 9a), which led to the conclusion that the current systems were highly structured (Figure 9b) [*Mauk and Saur*, 2007]. At Saturn (Figure 14d), equatorial electron beams have been observed as close to the planet as ~10 R_S, which led to the conclusion [*Saur et al.*, 2006] that at least some discrete auroral processes occur in regions much closer to Saturn than would be expected if the driver of auroral processes is primarily the divergence of flow in the vicinity of the boundary between open and closed field lines. Electron beams have been observed within the plasma wakes of both the Jupiter satellites Io (Figure 14b) and Callisto and have been attributed, again, to auroral current systems associated with the interactions between the conducting moons and the rapidly rotating magnetospheric plasmas (section 2.7) [*Williams et al.*, 1996, 1999; *Frank and Paterson*, 1999; *Mauk et al.*, 2001; *Mauk and Saur*, 2007]. More recently, they have been observed in the vicinity of Saturn's satellite Enceladus [*Pryor et al.*, 2011] (see section 2.7]. It would appear that the upward acceleration of electrons over a broad distribution of energies (not shown here) is a universal aspect of intense auroral processes wherever they occur. The differences are in the energies that are achieved. At Earth, energies up to 30 keV are reported, whereas at Saturn and Jupiter, energies >200 keV are common.

2.5.2. Ion Acceleration. At Earth, upgoing ion "conic" distributions are observed on high-latitude, low-altitude regions of the magnetic field lines that carry the upward electric currents and provide the downward accelerated electron distributions that generate intense aurora [*Shelley and Collin*, 1991; *Carlson et al.*, 1998]. Conic-shaped distributions result from low-altitude acceleration perpendicular to the magnetic field combined with the parallel acceleration that follows from the magnetic mirror force that pushes the particles into the distant magnetosphere. Only the Cassini mission has been at the right place with the right instrumentation to view such distributions at a nonterrestrial planet, Saturn (Figure 15) [*Mitchell et al.*, 2009b]. Here not only were very energetic

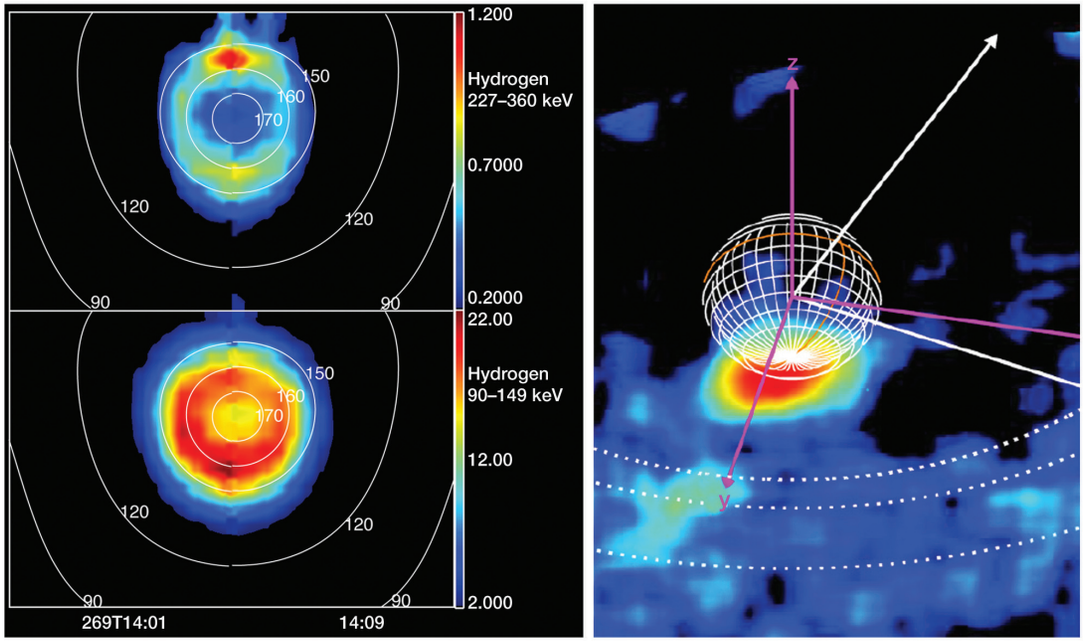

Figure 15. (left) A different representation of pitch angle distributions, this time for ions, where the white contours represent values of the pitch angle in degrees, and the colored intensities represent the intensity of the particle distributions at those pitch angles. Shown are upward propagating ion conic distributions measured at Saturn's high-latitude auroral regions. (right) Energetic neutral atom image of low-altitude auroral ion acceleration at Saturn's southern hemisphere. The bright region just under Saturn's southern pole likely represents the location of auroral acceleration, a conclusion supported by the fact that the ion emissions are protons or proton-related, without such heavy ions as oxygen or nitrogen observed elsewhere. From *Mitchell et al.* [2009b].

(~20 to >220 keV) upgoing ion conic distributions observed (Figure 15a), but the probable ion energization region was simultaneously imaged directly with energetic neutral atom imaging (Figure 15b). A significant difference between the observations at Earth and Saturn for the ions, as with the electrons, is the energies involved, with the Saturn ion conic energies extending up in energy by a factor of 20 to 100 higher than the same acceleration process operating at Earth.

2.6. Ionospheric Feedback

An important element in the auroral current system is the modification of the conductivity caused by the impact of accelerated charged particles onto the upper atmosphere. Such a modification can lead to a feedback process whereby an increase in auroral currents leads to an increase in conductivity, which in turn leads to further increases in auroral currents, etc. [*Watanabe and Sato*, 1988]. The importance of such a feedback process has not been established at Earth because its efficacy depends on the relative impedances of the magnetospheric current sources and the impedance of the ionosphere. These issues are addressed in section 3 and elsewhere in this volume. From a comparative standpoint, the role of the ionospheric response to auroral processes has recently been highlighted. One of the outstanding issues at Jupiter is why the magnetospheric plasmas continue to rotate at a substantial fraction of the planet's rotation rate to distances much larger than anticipated from core theoretical ideas involving plasma outflow, conservation of angular momentum, and uniform ionospheric conductivity [*Hill*, 1979; *Vasyliūnas*, 1983]. Increases to ionospheric conductivity are one way that the coupling between the planet and the distant space environment can be enhanced, thereby enhancing the rotational coupling [*Nichols and Cowley*, 2005]. *Ray et al.* [2010] and *Ray and Ergun* [this volume] describe a model that included both ionospheric conductivity enhancements and magnetic field-aligned electric fields and show that such effects can dramatically enhance rotational coupling.

The beauty of the Jupiter's auroral system compared with the system at Earth is that there is a very simple metric to test one's models: Do the model rotational flows at specified radial distances match the observations? While multiple processes can still influence the answer, leading to uncertainties remaining in the relative importance of those different processes, there exists no such simple metric at Earth. Jupiter provides an important test case.

2.7. Satellite Systems

One of the wonderful aspects of the nonterrestrial magnetospheric systems is the presence of electrically conducting

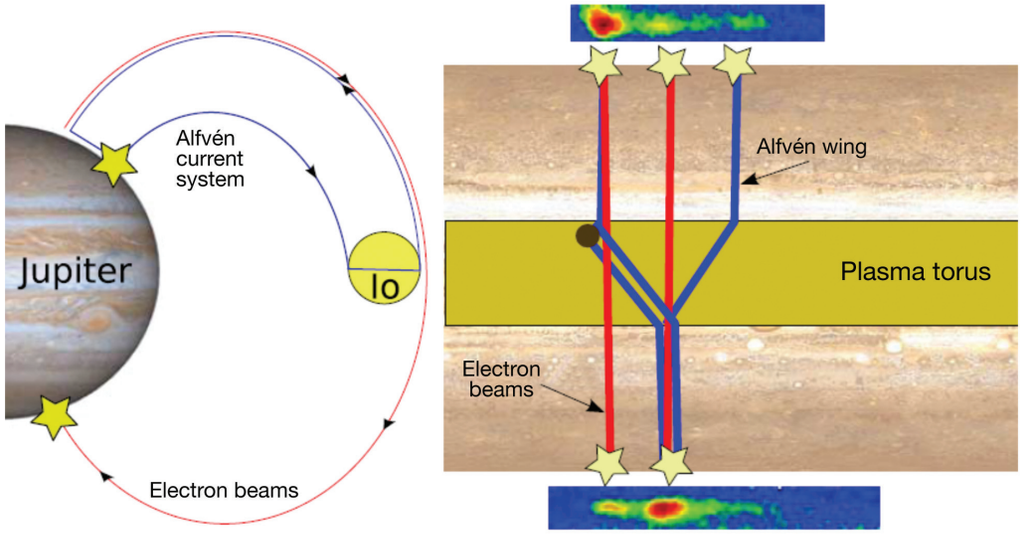

Figure 16. (top and bottom right) Images of northern and southern hemisphere auroral spots. The brightness of the spots as a function of position is interpreted on the basis of the Earth observations, whereby the brightest aurora emissions are generated by the downward acceleration of electrons in the upward (with respect to Jupiter) electric current regions, and the dimmer emissions are generated by the upward acceleration of electrons in the regions of downward electric currents. The upward accelerated electrons stimulate auroral emissions on the hemisphere opposite from where the acceleration occurred. Further details can be found in the source by *Bonfond et al.* [2008].

satellites that provide a whole new set of auroral systems. At Jupiter, auroral emissions are observed at the Jupiter magnetic foot points of the satellites Io (see Figure 1), Europa, and Ganymede [*Clarke et al.*, 2002; *Bonfond*, this volume; *Hess and Delamere*, this volume], and strong magnetic field-aligned electron beams were observed in the wake of Jupiter's satellite Callisto, indicative of the existence of an auroral current system, but with auroral emissions perhaps too weak to observe [*Mauk and Saur*, 2007], particularly occurring among the strong main auroral emissions. The electron beams observed near Callisto are similar to those observed in the plasma wake of Io (Figure 14b).

A highly significant finding (Figure 16) was reported by *Bonfond et al.* [2008], where direct evidence was discovered of the consequences of downward electron acceleration (in what is believed to be the upward current region) generating intense auroral emission associated with the satellite Io and the simultaneous generation of upward acceleration electrons (in the region of downward currents) generating auroral emissions in the opposite hemisphere. The ordering of the auroral phenomena engendered by the rapid rotation of the planet seems to provide a cleaner slate in sorting out the various mechanisms associated with the generation of auroral emissions than do the more chaotic conditions at Earth (Figure 4).

The satellite Enceladus at Saturn also generates a small-scale auroral current system [*Pryor et al.*, 2011] as illustrated in Figure 17 (Figure 17 was generated and provided by A. M. Rymer; the Enceladus spot is also highlighted in Figure 1). The inserted particle distribution (elevated above Enceladus) shows an upward (from Saturn) ion beaming distribution that was anticipated from the Earth aurora and from recent global auroral observations at Saturn (section 2.5), but that has not been reported in association with the other satellite interaction measurements. *Gurnett and Pryor* [this volume] report on other details of the Enceladus interactions.

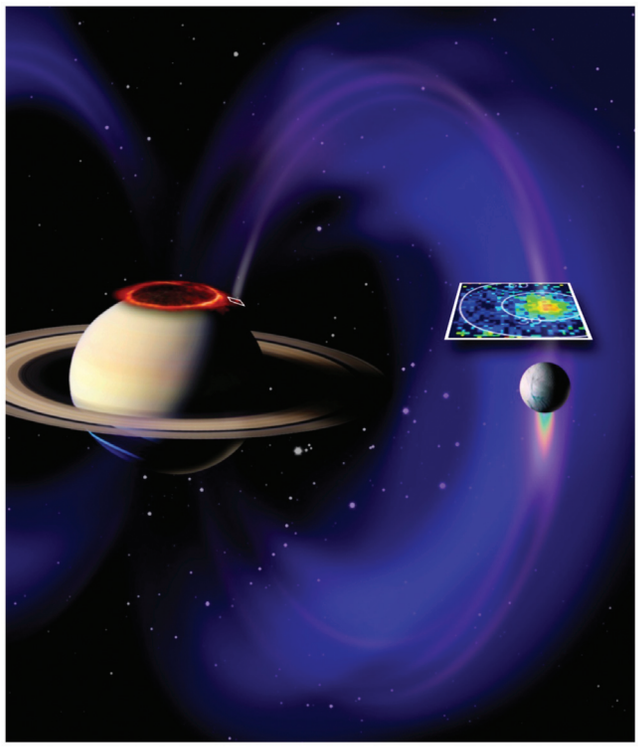

Figure 17. Auroral emissions measured by the Cassini UVIS instrument remapped onto visible image of Saturn and placed within the context of an artist's conception of the interaction between Saturn and Saturn's moon Enceladus, including an artist's conception of the gas and dust plumes coming out of Enceladus' southern polar regions. Levitated above Enceladus is a measured pitch angle distribution of the ion distributions that have been observed over Enceladus' polar regions (see the caption to Figure 15 for an explanation of the inserted pitch angle distribution). This figure was generated and provided by A. M. Rymer to highlight the discovery of the auroral spot at Saturn generated by the interaction sketched here. This discovery is reported by *Pryor et al.* [2011].

2.8. Other Processes

With this brief review, we have been able to compare only limited aspects of auroral phenomena among the different magnetized planets. A most glaring omission is our failure to address plasma wave and radio wave emission processes that are directly associated with auroral acceleration. Voyager epoch comparisons of plasma waves measured at Earth and on the nonterrestrial planets were performed by *Kurth and Gurnett* [1991]. Radio and plasma waves specific to auroral processes at Jupiter are discussed by *Clarke et al.* [2004], and those specific to Saturn are discussed by *Kurth et al.* [2009] and *Mauk et al.* [2009], and in all of these discussions, comparisons between the different planets are discussed. We recommend these and other sources to the reader. Our discussions of the upper atmospheric and ionospheric consequences of auroral processes have also been minimal at best. Several articles in the *Geophysical Monograph 130* [*Mendillo et al.*, 2002] provide the reader with reasonable starting points.

3. CONCLUSIONS

From observations taken to date, a preliminary conclusion can be drawn. When magnetospheric processes generate more electric current along magnetic field lines than can be carried by the existing populations, the response of the space environment appears to be at least superficially similar between the very different planetary systems: generation of

magnetic field-aligned electrical impedance, parallel electric fields, particle acceleration, auroral emissions, ionospheric modification, and momentum coupling between the upper atmosphere and the space environment. This conclusion, however, must remain preliminary until spacecraft have been able to probe the regions below the auroral acceleration region at a system other than the Earth. That is a prime objective of the late phase of the Cassini mission at Saturn and the Juno mission at Jupiter. The large differences among the various systems appear to be in the mechanisms by which the global system of electric currents is generated. Of course, there remain great uncertainties and controversies about how those current systems are generated, as other chapters in this volume demonstrate.

REFERENCES

Akasofu, S.-I., A. T. Y. Lui, and C.-I. Meng (2010), Importance of auroral features in the search for substorm onset processes, *J. Geophys. Res.*, *115*, A08218, doi:10.1029/2009JA014960.

Axford, W. I., and C. O. Hines (1961), A unifying theory of high-latitude geophysical phenomena and geomagnetic storms, *Can. J. Phys.*, *39*, 1433–1464.

Badman, S. V., and S. W. H. Cowley (2007), Significance of Dungey-cycle flows in Jupiter's and Saturn's magnetospheres, and their identification on closed equatorial field lines, *Ann. Geophys.*, *25*, 941–951.

Bagenal, F. (2009), Comparative planetary environments, in *Heliophysics: Plasma Physics of the Local Cosmos*, edited by C. J. Schrijver and G. L. Siscoe, pp. 360–398, Cambridge Univ. Press, New York.

Bagenal, F., and P. A. Delamere (2011), Flow of mass and energy in the magnetospheres of Jupiter and Saturn, *J. Geophys. Res.*, *116*, A05209, doi:10.1029/2010JA016294.

Belcher, J. W., R. L. McNutt Jr., J. D. Richardson, R. S. Selesnick, E. C. Sittler Jr., and F. Bagenal (1991), The plasma environment of Uranus, in *Uranus*, edited by J. T. Bergstrahl, E. D. Miner, and M. S. Matthews, p. 780, Univ. of Ariz. Press, Tucson.

Bishop, J., S. K. Atreya, P. N. Romani, G. S. Orton, B. R. Sandel, and R. V. Yelle (1995), The middle and upper atmosphere of Neptune, in *Neptune and Triton*, edited by D. P. Cruikshank, pp. 427–487, Univ. of Ariz. Press, Tucson.

Bonfond, B. (2012), When moons create aurora: The satellite footprints on giant planets, in *Auroral Phenomenology and Magnetospheric Processes: Earth and Other Planets*, *Geophys. Monogr. Ser.*, doi:10.1029/2011GM001169, this volume.

Bonfond, B., D. Grodent, J.-C. Gérard, A. Radioti, J. Saur, and S. Jacobsen (2008), UV Io footprint leading spot: A key feature for understanding the UV Io footprint multiplicity?, *Geophys. Res. Lett.*, *35*, L05107, doi:10.1029/2007GL032418.

Borovsky, J. E. (1993), Auroral arc thicknesses as predicted by various theories, *J. Geophys. Res.*, *98*(A4), 6101–6138.

Brain, D., and J. S. Halekas (2012), Aurora in Martian minimagnetospheres, in *Auroral Phenomenology and Magnetospheric Processes: Earth and Other Planets*, *Geophys. Monogr. Ser.*, doi:10.1029/2011GM001200, this volume.

Brice, N. M. (1967), Bulk motion of the magnetosphere, *J. Geophys. Res.*, *72*(21), 5193–5211.

Brice, N. M., and G. A. Ioannidis (1970), The magnetospheres of Jupiter and Earth, *Icarus*, *13*(2), 173–183, doi:10.1016/0019-1035(70)90048-5.

Bunce, E. J. (2012), Origins of Saturn's auroral emissions and their relationship to large-scale magnetosphere dynamics, in *Auroral Phenomenology and Magnetospheric Processes: Earth and Other Planets*, *Geophys. Monogr. Ser.*, doi:10.1029/2011GM001191, this volume.

Bunce, E. J., et al. (2008), Origin of Saturn's aurora: Simultaneous observations by Cassini and the Hubble Space Telescope, *J. Geophys. Res.*, *113*, A09209, doi:10.1029/2008JA013257.

Carlson, C. W., et al. (1998), FAST observations in the downward auroral current region: Energetic upgoing electron beams, parallel potential drops, and ion heating, *Geophys. Res. Lett.*, *25*(12), 2017–2020.

Chaston, C. C., J. W. Bonnell, C. W. Carlson, J. P. McFadden, R. E. Ergun, and R. J. Strangeway (2003), Properties of small-scale Alfvén waves and accelerated electrons from FAST, *J. Geophys. Res.*, *108*(A4), 8003, doi:10.1029/2002JA009420.

Chen, A. J. (1970), Penetration of low-energy protons deep into the magnetosphere, *J. Geophys. Res.*, *75*(13), 2458–2467.

Clarke, J. T. (2012), Auroral processes on Jupiter and Saturn, in *Auroral Phenomenology and Magnetospheric Processes: Earth and Other Planets*, *Geophys. Monogr. Ser.*, doi:10.1029/2011GM001199, this volume.

Clarke, J. T., et al. (2002), Ultraviolet emissions from the magnetic footprints of Io, Ganymede, and Europa on Jupiter, *Nature*, *415*, 997–1000.

Clarke, J. T., D. Grodent, S. W. H. Cowley, E. J. Bunce, P. Zarka, J. E. P. Connerney, and T. Satoh (2004), Jupiter's aurora, in *Jupiter: The Planet, Satellites and Magnetosphere*, edited by F. Bagenal, T. E. Dowling, and W. B. McKinnon, pp. 639–670, Cambridge Univ. Press, New York.

Cowley, S. W. H. (2000), Magnetosphere-ionosphere interactions: A tutorial review, in *Magnetospheric Current Systems*, *Geophys. Monogr. Ser.*, vol. 118, edited by S. Ohtani et al., pp. 91–106, AGU, Washington, D. C., doi:10.1029/GM118p0091.

Cowley, S. W. H., and E. J. Bunce (2001), Origin of the main auroral oval in Jupiter's coupled magnetosphere-ionosphere system, *Planet. Space Sci.*, *49*, 1067–1088.

Cowley, S. W. H., E. J. Bunce, T. S. Stallard, and S. Miller (2003), Jupiter's polar ionospheric flows: Theoretical interpretation, *Geophys. Res. Lett.*, *30*(5), 1220, doi:10.1029/2002GL016030.

Cowley, S. W. H., E. J. Bunce, and J. M. O'Rourke (2004), A simple quantitative model of plasma flows and currents in Saturn's polar ionosphere, *J. Geophys. Res.*, *109*, A05212, doi:10.1029/2003JA010375.

Delamere, P. A. (2012), Auroral signatures of solar wind interaction at Jupiter, in *Auroral Phenomenology and Magnetospheric Processes: Earth and Other Planets*, *Geophys. Monogr. Ser.*, doi:10.1029/2011GM001180, this volume.

Delamere, P. A., and F. Bagenal (2010), Solar wind interaction with Jupiter's magnetosphere, *J. Geophys. Res.*, *115*, A10201, doi:10.1029/2010JA015347.

Donovan, E., E. Spanswick, J. Liang, J. Grant, B. Jackel, and M. Greffen (2012), Magnetospheric dynamics and the proton aurora, in *Auroral Phenomenology and Magnetospheric Processes: Earth and Other Planets*, *Geophys. Monogr. Ser.*, doi:10.1029/2011GM001241, this volume.

Elphic, R. C., et al. (1998), The auroral current circuit and field-aligned currents observed by FAST, *Geophys. Res. Lett.*, *25*(12), 2033–2036.

Ergun, R. E., et al. (1998), FAST satellite observations of electric field structures in the auroral zone, *Geophys. Res. Lett.*, *25*(12), 2025–2028.

Feynman, R. P., R. B. Leighton, and M. Sands (1964), *The Feynman Lectures on Physics*, vol. 2, Addison-Wesley, Reading, Mass.

Fowles, G. R., and G. L. Cassiday (1993), *Analytical Mechanics*, 5th ed., W. B. Saunders, Philadelphia, Pa.

Frank, L. A., and J. D. Craven (1988), Imaging results from Dynamics Explorer 1, *Rev. Geophys.*, *26*(2), 249–283.

Frank, L. A., and W. R. Paterson (1999), Intense electron beams observed at Io with the Galileo spacecraft, *J. Geophys. Res.*, *104*(A12), 28,657–28,669, doi:10.1029/1999JA900402.

Frank, L. A., and W. R. Paterson (2002), Galileo observations of electron beams and thermal ions in Jupiter's magnetosphere and their relationship to the auroras, *J. Geophys. Res.*, *107*(A12), 1478, doi:10.1029/2001JA009150.

Frank, L. A., and W. R. Paterson (2004), Plasmas observed near local noon in Jupiter's magnetosphere with the Galileo spacecraft, *J. Geophys. Res.*, *109*, A11217, doi:10.1029/2002JA009795.

Gorney, D. J. (1991), An overview of auroral spatial scales, in *Auroral Physics*, edited by C.-I. Meng et al., p. 325, Cambridge Univ. Press, New York.

Gurnett, D. A., and W. R. Pryor (2012), Auroral processes associated with Saturn's moon Enceladus, in *Auroral Phenomenology and Magnetospheric Processes: Earth and Other Planets*, *Geophys. Monogr. Ser.*, doi:10.1029/2011GM001174, this volume.

Herbert, F. (2009), Aurora and magnetic field of Uranus, *J. Geophys. Res.*, *114*, A11206, doi:10.1029/2009JA014394.

Herbert, F., and B. R. Sandel (1994), The Uranian aurora and its relationship to the magnetosphere, *J. Geophys. Res.*, *99*(A3), 4143–4160.

Hess, S. L. G., and P. A. Delamere (2012), Satellite-induced electron acceleration and related auroras, in *Auroral Phenomenology and Magnetospheric Processes: Earth and Other Planets*, *Geophys. Monogr. Ser.*, doi:10.1029/2011GM001175, this volume.

Hill, T. W. (1979), Inertial limit on corotation, *J. Geophys. Res.*, *84*(A11), 6554–6558.

Hill, T. W. (2001), The Jovian auroral oval, *J. Geophys. Res.*, *106*(A5), 8101–8107, doi:10.1029/2000JA000302.

Horne, R. B., R. M. Thorne, N. P. Meredith, and R. R. Anderson (2003), Diffuse auroral electron scattering by electron cyclotron harmonic and whistler mode waves during an isolated substorm, *J. Geophys. Res.*, *108*(A7), 1290, doi:10.1029/2002JA009736.

Kavanagh, L. D., Jr., J. W. Freeman Jr., and A. J. Chen (1968), Plasma flow in the magnetosphere, *J. Geophys. Res.*, *73*(17), 5511–5519.

Keiling, A. (2009), Alfvén waves and their roles in the dynamics of the Earth's magnetotail: A review, *Space Sci. Rev.*, *142*(1–4), 73–156.

Keiling, A., J. R. Wygant, C. Cattell, W. Peria, G. Parks, M. Temerin, F. S. Mozer, C. T. Russell, and C. A. Kletzing (2002), Correlation of Alfvén wave Poynting flux in the plasma sheet at 4–7 R_E with ionospheric electron energy flux, *J. Geophys. Res.*, *107*(A7), 1132, doi:10.1029/2001JA900140.

Keiling, A., J. R. Wygant, C. A. Cattell, F. S. Mozer, and C. T. Russell (2003), The global morphology of wave Poynting flux: Powering the aurora, *Science*, *299*, 383–386.

Keiling, A., et al. (2009), Substorm current wedge driven by plasma flow vortices: THEMIS observations, *J. Geophys. Res.*, *114*, A00C22, doi:10.1029/2009JA014114. [Printed 115(A1), 2010].

Kelley, M. C., D. J. Knudsen, and J. F. Vickrey (1991), Poynting flux measurements on a satellite: A diagnostic tool for space research, *J. Geophys. Res.*, *96*(A1), 201–207.

Klumpar, D. M., J. M. Quinn, and E. G. Shelley (1988), Counter-streaming electrons at the geomagnetic equator near 9 R_E, *Geophys. Res. Lett.*, *15*(11), 1295–1298.

Kurth, W. S., and D. A. Gurnett (1991), Plasma waves in planetary magnetospheres, *J. Geophys. Res.*, *96*, 18,977–18,991.

Kurth, W. S., et al. (2009), Auroral processes, in *Saturn from Cassini-Huygens*, edited by M. Dougherty, L. Esposito and S. Krimigis, p. 333, Springer, New York.

Lessard, M. R. (2012), A review of pulsating aurora, in *Auroral Phenomenology and Magnetospheric Processes: Earth and Other Planets*, *Geophys. Monogr. Ser.*, doi:10.1029/2011GM001187, this volume.

Li, W., J. Bortnik, Y. Nishimura, R. M. Thorne, and V. Angelopoulos (2012), The origin of pulsating aurora: Modulated whistler mode chorus waves, in *Auroral Phenomenology and Magnetospheric Processes: Earth and Other Planets*, *Geophys. Monogr. Ser.*, doi:10.1029/2011GM001192, this volume.

Lundin, R., G. Haerendel, and S. Grahn (1998), Introduction to special section: The Freja Mission, *J. Geophys. Res.*, *103*(A3), 4119–4123.

Lyons, L. R., Y. Nishimura, Y. Shi, S. Zou, H.-J. Kim, V. Angelopoulos, C. Heinselman, M. J. Nicolls, and K.-H. Fornacon (2010), Substorm triggering by new plasma intrusion: Incoherent-scatter radar observations, *J. Geophys. Res.*, *115*, A07223, doi:10.1029/2009JA015168.

Lyons, L. R., Y. Nishimura, X. Xing, Y. Shi, M. Gkioulidou, C.-P. Wang, H.-J. Kim, S. Zou, V. Angelopoulos, and E. Donovan (2012), Auroral disturbances as a manifestation of interplay between large-scale and mesoscale structure of

magnetosphere-ionosphere electrodynamical coupling, in *Auroral Phenomenology and Magnetospheric Processes: Earth and Other Planets*, *Geophys. Monogr. Ser.*, doi:10.1029/2011GM001152, this volume.

Lysak, R. L. (Ed.) (1993), *Auroral Plasma Dynamics*, *Geophys. Monogr. Ser.*, vol. 80, 291 pp., AGU, Washington D. C., doi:10.1029/GM080.

Mauk, B. H., and N. J. Fox (2010), Electron radiation belts of the solar system, *J. Geophys. Res.*, *115*, A12220, doi:10.1029/2010JA015660.

Mauk, B. H., and S. M. Krimigis (1987), Radial force balance within Jupiter's dayside magnetosphere, *J. Geophys. Res.*, *92*(A9), 9931–9941.

Mauk, B. H., and C.-I. Meng (1991), The aurora and middle magnetospheric processes, in *Auroral Physics*, edited by C.-I. Meng et al., p. 223, Cambridge Univ. Press, Cambridge, U. K.

Mauk, B. H., and J. Saur (2007), Equatorial electron beams and auroral structuring at Jupiter, *J. Geophys. Res.*, *112*, A10221, doi:10.1029/2007JA012370.

Mauk, B. H., S. M. Krimigis, E. P. Keath, A. F. Cheng, T. P. Armstrong, L. J. Lanzerotti, G. Gloeckler, and D. C. Hamilton (1987), The hot plasma and radiation environment of the Uranian magnetosphere, *J. Geophys. Res.*, *92*(A13), 15,283–15,308.

Mauk, B. H., D. J. Williams, and A. Eviatar (2001), Understanding Io's space environment interaction: Recent energetic electron measurements from Galileo, *J. Geophys. Res.*, *106*(A11), 26,195–26,208, doi:10.1029/2000JA002508.

Mauk, B. H., B. J. Anderson, and R. M. Thorne (2002a), Magnetosphere-ionosphere coupling at Earth, Jupiter, and beyond, in *Atmospheres in the Solar System: Comparative Aeronomy*, *Geophys. Monogr. Ser.*, vol. 130, edited by M. Mendillo, A. Nagy, and J. H. White, pp. 97–114, AGU, Washington, D. C., doi:10.1029/130GM07.

Mauk, B. H., J. T. Clarke, D. Grodent, J. H. Waite Jr., C. P. Paranicas, and D. J. Williams (2002b), Transient aurora on Jupiter from injections of magnetospheric electrons, *Nature*, *415*, 1003–1005.

Mauk, B. H., et al. (2009), Fundamental plasma processes in Saturn's magnetosphere, in *Saturn from Cassini-Huygens*, edited by M. Dougherty, L. Esposito and S. Krimigis, p. 281, Springer, New York.

McComas, D. J., and F. Bagenal (2007), Jupiter: A fundamentally different magnetospheric interaction with the solar wind, *Geophys. Res. Lett.*, *34*, L20106, doi:10.1029/2007GL031078.

McIlwain, C. E. (1975), Equatorial electron beams near the magnetic equator, in *The Physics of Hot Plasma in the Magnetosphere*, edited by B. Hultqvist and L. Stenflo, p. 91, Plenum, New York.

Mendillo, M., A. Nagy, and J. H. White (Eds.) (2002), *Atmospheres in the Solar System: Comparative Aeronomy*, *Geophys. Monogr. Ser.*, vol. 130, 388 pp., AGU, Washington, D. C., doi:10.1029/GM130.

Meredith, N. P., R. B. Horne, R. M. Thorne, and R. R. Anderson (2009), Survey of upper band chorus and ECH waves: Implications for the diffuse aurora, *J. Geophys. Res.*, *114*, A07218, doi:10.1029/2009JA014230.

Mitchell, D. G., et al. (2009a), Recurrent energization of plasma in the midnight-to-dawn quadrant of Saturn's magnetosphere, and its relationship to auroral UV and radio emissions, *Planet. Space Sci.*, *57*, 1732–1742.

Mitchell, D. G., W. S. Kurth, G. B. Hospodarsky, N. Krupp, J. Saur, B. H. Mauk, J. F. Carbary, S. M. Krimigis, M. K. Dougherty, and D. C. Hamilton (2009b), Ion conics and electron beams associated with auroral processes on Saturn, *J. Geophys. Res.*, *114*, A02212, doi:10.1029/2008JA013621.

Nagai, T., M. Fujimoto, R. Nakamura, W. Baumjohann, A. Ieda, I. Shinohara, S. Machida, Y. Saito, and T. Mukai (2005), Solar wind control of the radial distance of the magnetic reconnection site in the magnetotail, *J. Geophys. Res.*, *110*, A09208, doi:10.1029/2005JA011207.

Newell, P. T., T. Sotirelis, and S. Wing (2009), Diffuse, monoenergetic, and broadband aurora: The global precipitation budget, *J. Geophys. Res.*, *114*, A09207, doi:10.1029/2009JA014326.

Ni, B., R. M. Thorne, Y. Y. Shprits, and J. Bortnik (2008), Resonant scattering of plasma sheet electrons by whistler-mode chorus: Contribution to diffuse auroral precipitation, *Geophys. Res. Lett.*, *35*, L11106, doi:10.1029/2008GL034032.

Nichols, J. D., and S. W. H. Cowley (2005), Magnetosphere-ionosphere coupling currents in Jupiter's middle magnetosphere: Effect of magnetosphere-ionosphere decoupling by field-aligned auroral voltages, *Ann. Geophys.*, *23*, 799–808.

Nishida, A. (1966), Formation of plasmapause, or magnetospheric plasma knee, by the combined action of magnetospheric convection and plasma escape from the tail, *J. Geophys. Res.*, *71*(23), 5669–5679.

Nishimura, Y., et al. (2010), Preonset time sequence of auroral substorms: Coordinated observations by all-sky imagers, satellites, and radars, *J. Geophys. Res.*, *115*, A00I08, doi:10.1029/2010JA015832. [Printed 116(A5), 2011].

Paranicas, C. P., B. H. Mauk, and S. M. Krimigis (1991), Pressure anisotropy and radial stress balance in the Jovian neutral sheet, *J. Geophys. Res.*, *96*(A12), 21,135–21,140.

Parks, G. K. (1991), *Physics of Space Plasmas*, Westview, Cambridge, Mass.

Pryor, W. R., et al. (2011), The auroral footprint of Enceladus on Saturn, *Nature*, *472*, 331–333, doi:10.1038/nature09928.

Pu, Z. Y., et al. (2010), THEMIS observations of substorms on 26 February 2008 initiated by magnetotail reconnection, *J. Geophys. Res.*, *115*, A02212, doi:10.1029/2009JA014217.

Ray, L. C., and R. E. Ergun (2012), Auroral signatures of ionosphere-magnetosphere coupling at Jupiter and Saturn, in *Auroral Phenomenology and Magnetospheric Processes: Earth and Other Planets*, *Geophys. Monogr. Ser.*, doi:10.1029/2011GM001172, this volume.

Ray, L. C., R. E. Ergun, P. A. Delamere, and F. Bagenal (2010), Magnetosphere-ionosphere coupling at Jupiter: Effect of field-aligned potentials on angular momentum transport, *J. Geophys. Res.*, *115*, A09211, doi:10.1029/2010JA015423.

Saur, J., A. Pouquet, and W. H. Matthaeus (2003), An acceleration mechanism for the generation of the main auroral oval on Jupiter, *Geophys. Res. Lett.*, *30*(5), 1260, doi:10.1029/2002GL015761.

Saur, J., et al. (2006), Anti-planetward auroral electron beams at Saturn, *Nature*, *439*, 699–702, doi:10.1038/nature04401.

Schriver, D., M. Ashour-Abdalla, R. J. Strangeway, R. L. Richard, C. Klezting, Y. Dotan, and J. Wygant (2003), FAST/Polar conjunction study of field-aligned auroral acceleration and corresponding magnetotail drivers, *J. Geophys. Res.*, *108*(A9), 8020, doi:10.1029/2002JA009426.

Selesnick, R. S. (1990), Plasma convection in Neptune's magnetosphere, *Geophys. Res. Lett.*, *17*(10), 1681–1684.

Selesnick, R. S., and R. L. McNutt Jr. (1987), Voyager 2 plasma ion observations in the magnetosphere of Uranus, *J. Geophys. Res.*, *92*(A13), 15,249–15,262.

Shelley, E. G., and H. L. Collin (1991), Auroral ion acceleration and its relationship to ion composition, in *Auroral Physics*, edited by C.-I. Meng, M. J. Rycroft, and L. A. Frank, p. 129, Cambridge Univ. Press, New York.

Stasiewicz, K., et al. (2000), Small scale Alfvénic structure in the aurora, *Space Sci. Rev.*, *92*, 423–533.

Stern, D. P. (1984), Magnetospheric dynamo processes, in *Magnetospheric Currents*, *Geophys. Monogr. Ser.*, vol. 28, edited by T. A. Potemra, pp. 200–207, AGU, Washington, D. C., doi:10.1029/GM028p0200.

Su, Z., H. Zheng, and S. Wang (2010), A parametric study on the diffuse auroral precipitation by resonant interaction with whistler mode chorus, *J. Geophys. Res.*, *115*, A05219, doi:10.1029/2009JA014759.

Vasyliūnas, V. M. (1975), Concepts of magnetospheric convection, in *The Magnetospheres of the Earth and Jupiter*, edited by V. Formisano, p. 179, D. Reidel, Boston, Mass.

Vasyliūnas, V. M. (1983), Plasma distribution and flow, in *Physics of the Jovian Magnetosphere*, edited by A. J. Dessler, pp. 395–453, Cambridge Univ. Press, London, U. K.

Vasyliūnas, V. M. (2001), Electric field and plasma flow: What drives what?, *Geophys. Res. Lett.*, *28*(11), 2177–2180, doi:10.1029/2001GL013014.

Vasyliūnas, V. M. (2011), Physics of magnetospheric variability, *Space Sci. Rev.*, *158*, 91–118, doi:10.1007/s11214-010-9696-1.

Watanabe, K., and T. Sato (1988), Self-excitation of auroral arcs in a three-dimensionally coupled magnetosphere-ionosphere system, *Geophys. Res. Lett.*, *15*(7), 717–720.

Watt, C. E. J., and R. Rankin (2012), Alfvén wave acceleration of auroral electrons in warm magnetospheric plasma, in *Auroral Phenomenology and Magnetospheric Processes: Earth and Other Planets*, *Geophys. Monogr. Ser.*, doi:10.1029/2011GM001171, this volume.

Williams, D. J., B. H. Mauk, R. E. McEntire, E. C. Roelof, T. P. Armstrong, B. Wilken, J. G. Roederer, S. M. Krimigis, T. A. Fritz, and L. J. Lanzerotti (1996), Electron beams and ion composition measured at Io and in its torus, *Science*, *274*, 401–403.

Williams, D. J., R. M. Thorne, and B. Mauk (1999), Energetic electron beams and trapped electrons at Io, *J. Geophys. Res.*, *104*(A7), 14,739–14,753, doi:10.1029/1999JA900115.

Wygant, J. R., et al. (2000), Polar spacecraft based comparisons of intense electric fields and Poynting flux near and within the plasma sheet-tail lobe boundary to UVI images: An energy source for the aurora, *J. Geophys. Res.*, *105*(A8), 18,675–18,692, doi:10.1029/1999JA900500.

Wygant, J. R., et al. (2002), Evidence for kinetic Alfvén waves and parallel electron energization at 4–6 R_E altitudes in the plasma sheet boundary layer, *J. Geophys. Res.*, *107*(A8), 1201, doi:10.1029/2001JA900113.

Zhang, H., et al. (2007), TC-1 observations of flux pileup and dipolarization-associated expansion in the near-Earth magnetotail during substorms, *Geophys. Res. Lett.*, *34*, L03104, doi:10.1029/2006GL028326.

F. Bagenal, Laboratory for Space and Atmospheric Sciences, University of Colorado, Boulder, CO 80309, USA. (bagenal@colorado.edu)

B. Mauk, The Johns Hopkins University Applied Physics Laboratory, Laurel, MD 20723, USA. (Barry.Mauk@jhuapl.edu)